Beam Physics Note
TRI-BN-19-18R
September 3, 2019

Langevin-Like DTL Triplet BI Fits and Analysis of Transverse DTL Tuning Difficulties

Olivier Shelbaya, Rick Baartman

TRIUMF

Abstract: Triplets in the separated function ISAC Drift Tube Linac provide corrective transverse focussing, counteracting the accumulated effects of RF. In order to produce both reliable tuning procedures and in the interest of accelerator modelling, precise magnetic field characterizations are required. Using original magnetic field survey data, performed on each of the DTL triplet magnets circa 2000, a Langevin-like hyperbolic function is fit to the survey data in an attempt to provide a working BI relation for the ISAC DTL. An investigation into the DTL triplet currents provided to RIB Operations, circa 2002, is also performed, in addition to the identification of a potential RFQ to MEBT line misalignment. Evidence supporting the latter is discussed, likely explaining DTL tuning difficulties over the last years. The original DTL transverse tune is then successfully verified at Tank-2 energy.

4004 Wesbrook Mall, Vancouver, B.C. Canada V6T 2A3 Tel: 604 222-1047 www.triumf.ca

Contents

List of Figures

List of Tables

Prelude: Tuning the ISAC Drift Tube Linac Quadrupoles

> Energy Change complete, +5Ne-21 883KeV/u to Dragon. Roughly (numbers to follow) 80-85% transmission MEBT:FC9 to DRA:FCCH, with 100% from HEBT2:FC4 to DRA:FCCH. They are checking the energy with Neon beam, I requested protons back from Ops, they are just coming vback *(sic)* from a 2.5 hour fight with their RF. For anyone that cares, I set the energy's per Bob's note stuck to the Keithley, and made the beam look nice at the Prague harp using Tank 4 phase and amplitude. Once the RF was happy, I used HEBT->Dragon optics from a save Apr 29 at 12:18 when the energy was 877KeV/u and scaled it up. Tuned the DTL by hand from theoretical numbers from Matteo's spreadsheet and tweeked pretty much everything optics-wise. Save /b/020519_2050.snapiosdragon.
>
> Chris Payne, ISAC Operations e-log, May 19 2002

Over the years since the DTL was initially commissioned, operations have resorted to manually tuning the DTL triplets during accelerator setup, relying upon transmission as the main indicator of quality. A set of DTL triplet quadrupole setpoints, part of a spreadsheet provided to operations in the early 2000's, formed the initial basis of DTL tuning methodology. These spreadsheet magnet currents were known to require significant manual adjustment however, with entries in the ISAC Operations electronic logbook dating back to 2002 highlighting this fact, shown at the top of the present page.

As a consequence of the unreliability of the predicted magnet currents, tuning of the DTL quadrupoles was considered by ISAC Operations both a tedious and time consuming task. In particular, as operators tuned the DTL, after each tank and buncher was ramped to its design longitudinal energy, all downstream triplets required further retuning, in order to restore transmission, compensating for the new beam energy and associated RF defocussing. The spreadsheet numbers were eventually abandoned by both operators and physicists.

To attempt to palliate this issue, a running average of working DTL quadrupole currents was collected by the Beam Delivery group, associated with each A/q delivered to experiments. While these numbers, found laboriously by hand, trial and error, did aid in reducing the necessary setup time, they were never demonstrated to produce a satisfactory tune through simulations. As of early 2019, the time required to tune the DTL, including phasing tanks and adjusting the triplets was officially quoted as an entire 8-hour shift, imposing a considerable time-cost to tuning the accelerator.

The present note details a re-analysis of the original DTL quadrupole triplet survey data, dating back to 2000, in which each DTL triplet was surveyed on a static test bench by TRIUMF staff upon reception from the manufacturer. Following this analysis, a set of DTL triplet current setpoints was produced and ultimately tested with stable beam, on August 6th, 2019. A brief analysis of this beam test is presented, in addition to an investigation of the original DTL triplet currents which were provided to ISAC Operations no later than May 2002.

1 BI Fit Characterization

A good empirical fit can be obtained with only two parameters using the following function:

$$L(I) = \frac{a_1}{a_3} \tanh\left[a_3 I + \frac{1}{3}(a_3 I)^3 + \frac{1}{5}(a_3 I)^5\right] \tag{1}$$

We refer to this function as a 'pseudoLangevin'. The reason this works well is that the harmonic series with only odd terms, $x + x^3/3 + x^5/5 + ...$, is the series expansion of hyperbolic arctangent. Taking the tanh of an arctanh gives the function $f(x) = x$, but only up to $x = 1$. From that point onward, the series diverges and the tanh of infinity is 1. Thus for the infinite series, we have a linear function with a kink at 1 after which it stays at 1. Taking only one term, it's simply a tanh. As one takes progressively more terms the "knee" grows sharper. We have found that three terms works well, and is superior to polynomial fits in that it has correct saturating behaviour and requires fewer parameters.

The behavior exhibited by these functions is shown in Figure 1 for a few cases, including a 3 term series as shown in equation 1. This function has been fit to original DTL magnet triplet BI characterizations, performed by Doug Evans circa 2000, shortly after delivery of the triplet assemblies on site.

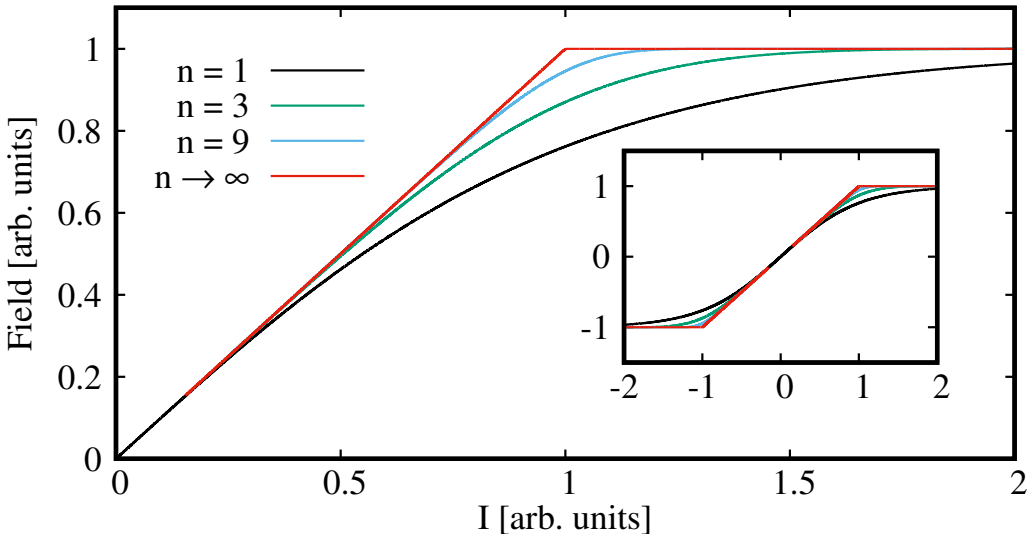

Figure 1: Unscaled pseudoLangevin (n = 3) BI function as shown in Eq. 1, with both fit parameters set to unity. For comparison, the values of the function $\tanh\left[\sum_{j=1,3,5,...}^{n} x^j/j\right]$ is shown for n = 1,3,9 and ∞, showing the limiting behavior of the function. The inset plot shows the same function's behavior over a symmetric negative interval, with identical x and y axis definitions, for the identical values of n.

2 Original Magnet Surveys

Magnetic field surveys were performed at TRIUMF shortly after reception of the triplet assemblies. The original data has been recovered and processed, shown in Appendix A. Figure 2 shows original aggregate BI values collected on all DTL quadrupole triplet magnets. In the figure, Q1-like quads denote all outer triplet magnets, while Q2-like corresponds to inner quadrupole magnets.

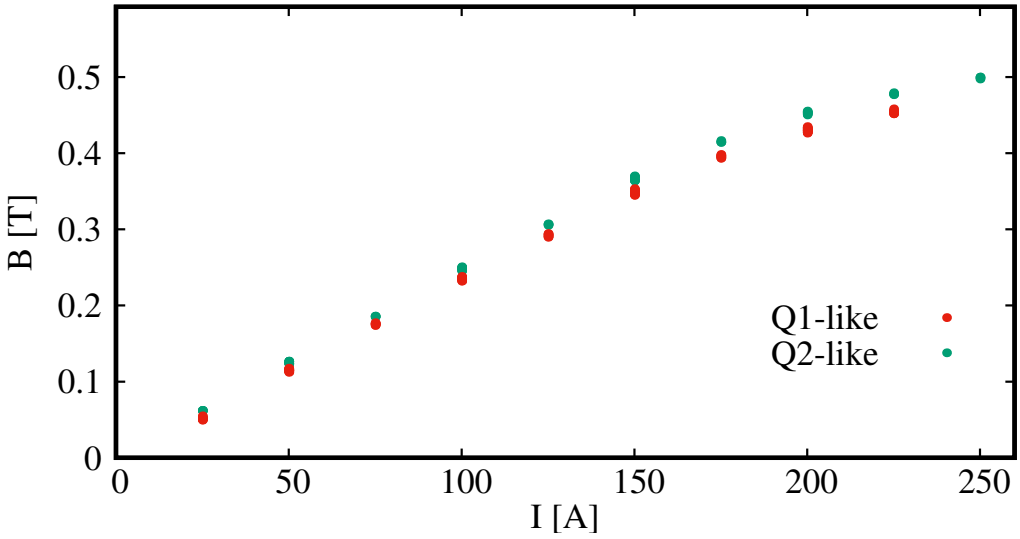

Figure 2: Original DTL triplet magnet survey data, collected by Doug Evans circa 2000, showing recorded quadrupole BI relationship for all DTL triplets. Q1-like magnets correspond to magnets on the outer triplet (Q1,Q3,Q4,Q6,etc..), while Q2-like denote the central triplet magnet. Note that the hall probe was placed at an off-axis displacement position of 0.236" = 0.599cm, corresponding to half the magnet bore radius. Note that the outer triplet surveys were performed up to I = 225A, while for the inner magnet it was taken to I = 250A.

It is noted that the magnet surveys used in the present work have all been performed by placing the survey probe at a bore radius position of 0.236" = 0.599cm, corresponding to half the DTL quadrupole magnet aperture radius of 0.472" = 1.199cm. As such, it is expected from the triplet design that the pole-tip field should scale by a factor of 0.472"/0.236" = 2.

3 Hyperbolic Fits

The raw survey data was fit to Eq. 1 for the aggregate data shown in Fig. 2, using a nonlinear least-squares algorithm, producing fit parameters shown in Table 1. The fit routine outputs are shown in appendices B and C. Two separate fits were performed, one for Q1-like and one for Q2-like magnets. The parameters a_1 in Table 1 have been scaled by a factor of 2. The unscaled fits are shown overlaid with the original survey data in Fig. 3 and 4, along with the residual fit error, namely due to hysteresis, shown in the same figures.

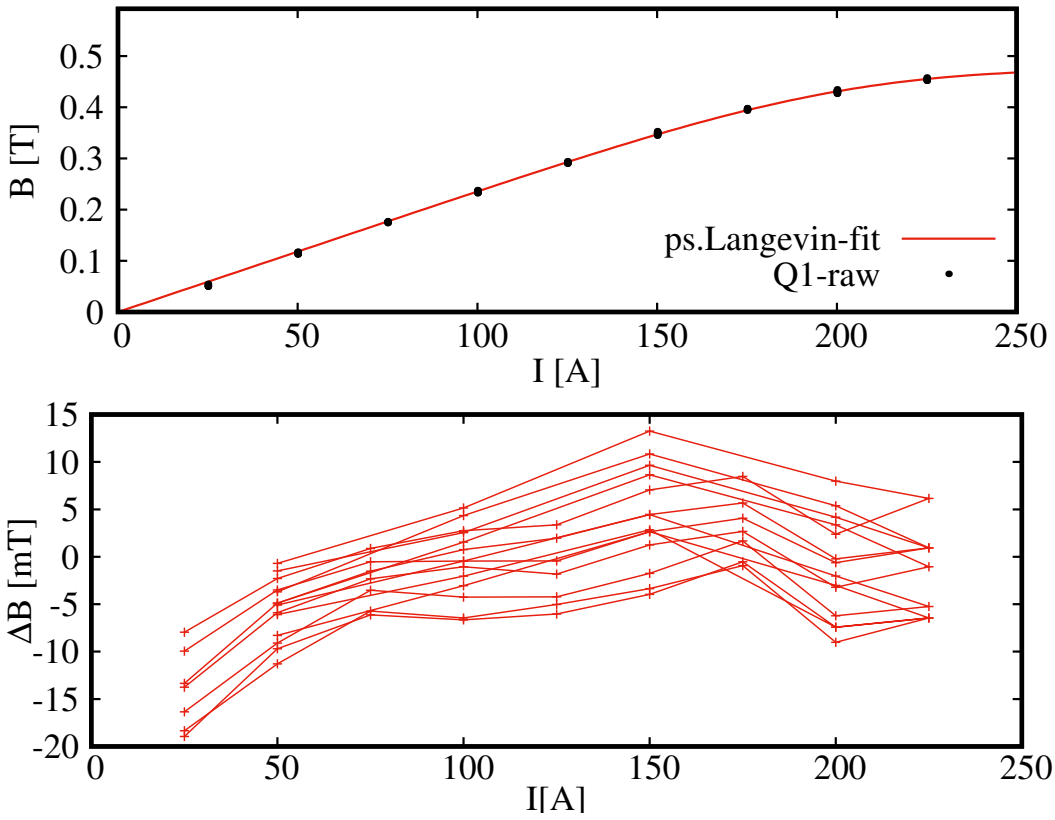

Figure 3: **Top:** pseudoLangevin function fits to DTL triplet magnet BI survey data, using Eq. 1 for Q1-like (outer) triplet quadrupoles. **Bottom:** Deviation between pseudoLangevin and raw data, with lines joining datapoints in order of collection, showing effects of hysteresis. **note: raw bi data collected at r = 0.236", being the half-bore radius point, as shown in the above figures. parameter $\mathrm{a_1}$ is half what is shown in Table 1.**

Inspection of the magnetic field deviation between pseudoLangevin fits and the raw survey data reveals an absolute field error peaking at almost 20 mT for the 25A measurements for the Q1-like quadrupoles in Figure 3, absent in Figure 4. While the precise reason for this disagreement is at present unknown, it is important to note that the percent deviations for typical operating currents, usually in the 100A range, remain well bounded below an absolute error value of roughly 3%. The latter error may be attributed to hysteresis effects.

Parameter	Q1-like	Q2-like
$a_1[\mathrm{T/A}]$	$(4.718\pm0.008)\times10^{-3}$	$(4.961\pm0.008)\times10^{-3}$
$a_3^{-1}[\mathrm{A}]$	201.1 ± 0.9	202.7 ± 0.7

Table 1: BI Fit parameters for Eq. 1 for both Q1 and Q2-type magnets. **Note: these parameters have been scaled to give the pole-tip field at the magnet bore radius.**

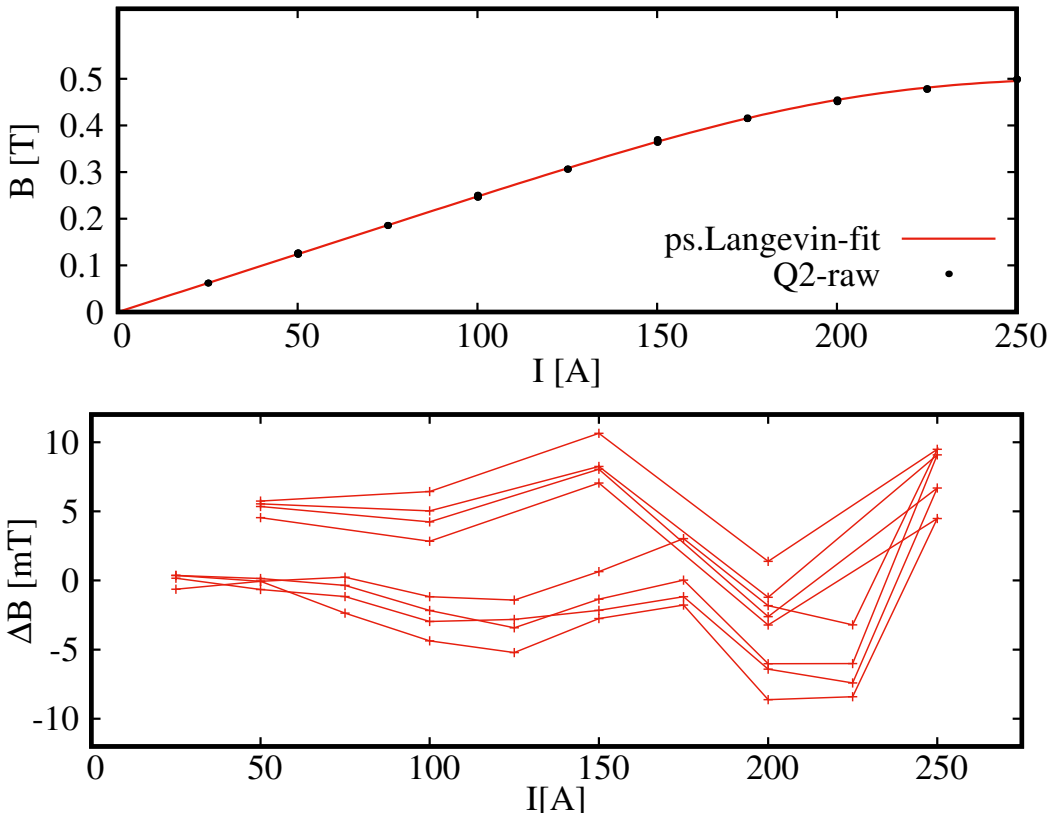

Figure 4: **Top:** pseudoLangevin function fits to DTL triplet magnet BI survey data, using Eq. 1 for q2-like (inner) quadrupoles. **Bottom:** Deviation between pseudoLangevin and raw data, with lines joining datapoints in order of collection, showing effects of hysteresis. **Note: raw BI data collected at r = 0.236", being the half-bore radius point, as shown in the above figures. Parameter a_1 is half what is shown in Table 1.**

4 Recalling the DTL Design Tune

Original transverse focussing specifications for the DTL were computed using the particle tracking code LANA, including magnet effective length and strength requirements [1]. As the DTL frequency and energy profile converged to its final and present form, the required first order corrective transverse gradients were obtained, providing the basis for the design requirements of the DTL triplets, shown in Table 2. It is noted that these numbers correspond to the 105 MHz DTL tune, not the final 106.08 MHz, which arose as a consequence of the ISAC-RFQ's 35.36 MHz, instead of 35.0 MHz resonant frequency. As the DTL is intended to operate at the third harmonic of the RFQ frequency, the DTL operating frequency had to be correspondingly adjusted.

The numbers shown in Table 2 have formed the theoretical grounding for ISAC/RIB Operations DTL tuning procedures and methodologies, going back to at least 2002. These numbers remained in use by operations until 2017, when the Beam Delivery group started relying upon manually defined

working tunes. For convenience, all values in Table 2 have been converted to pole-tip fields, shown in Table 3.

E [MeV/u]	0.236	0.440	0.781	1.148	1.50
Quad	G [T/m]	G [T/m]	G [T/m]	G [T/m]	G [T/m]
Q1	−53.1	−53.7	−53.7	−53.7	−53.7
Q2	46.6	48.6	48.6	48.6	48.6
Q3	−41.7	−47.1	−47.1	−47.1	−47.1
Q4	33.4	46.1	48.9	48.9	48.9
Q5	−36.3	−50.9	−54.0	−54.0	−54.0
Q6	30.4	43.7	48.9	48.9	48.9
Q7	−28.6	−40.3	−51.7	−55.3	−55.3
Q8	32.6	46.0	59.8	63.9	63.9
Q9	−26.6	−38.1	−49.5	−55.2	−55.2
Q10	23.7	35.9	48.3	53.6	54.7
Q11	−30.0	−43.1	−57.8	−62.5	−64.4
Q12	25.6	36.4	48.6	48.1	50.8

Table 2: Specifications for DTL quadrupole triplet gradient requirements for A/q = 6, obtained from [1]. **Note: A 105 MHz DTL-`LANA` simulation was used to derive the above numbers.**

E [MeV/u]	0.236	0.440	0.781	1.148	1.50
Quad	B_t [T]	B_t [T]	B_t [T]	B_t [T]	B_t [T]
Q1	−0.637	−0.644	−0.644	−0.644	−0.644
Q2	0.559	0.583	0.583	0.583	0.583
Q3	−0.500	−0.565	−0.565	−0.565	−0.565
Q4	0.400	0.553	0.586	0.586	0.586
Q5	−0.435	−0.610	−0.647	−0.647	−0.647
Q6	0.364	0.524	0.586	0.586	0.586
Q7	−0.343	−0.483	−0.620	−0.663	−0.663
Q8	0.391	0.551	0.717	0.766	0.766
Q9	−0.319	−0.457	−0.593	−0.662	−0.662
Q10	0.284	0.430	0.579	0.643	0.656
Q11	−0.360	−0.517	−0.693	−0.749	−0.772
Q12	0.307	0.436	0.583	0.577	0.609

Table 3: Converted DTL quadrupole triplet pole-tip magnetic field requirements for A/q = 6, derived from [1]. A magnet bore radius of r = 0.472”, obtained from DTL design drawing `IRF1002D.dwg`. **Note: A 105 MHz DTL-`LANA` simulation was used to derive the above numbers.**

Using Eq. 1 with the parameters listed in Table 1, the quadrupole currents associated with the pole tip field values in Table 3 were computed, by using a monte-carlo bisection method. The results are shown in Table 4.

E [MeV/u]	0.236	0.440	0.781	1.148	1.50
Quad	I [A]	I [A]	I [A]	I [A]	I [A]
Q1	136.57	138.23	138.23	138.23	138.23
Q2	113.05	118.03	118.03	118.03	118.03
Q3	106.26	120.39	120.39	120.39	120.39
Q4	84.93	117.75	125.17	125.17	125.17
Q5	87.79	123.81	131.72	131.72	131.72
Q6	77.28	111.46	125.17	125.17	125.17
Q7	72.69	102.64	132.73	142.71	142.71
Q8	78.81	111.56	147.06	158.55	158.55
Q9	67.60	96.97	126.78	142.43	142.43
Q10	60.22	91.33	123.57	137.95	141.02
Q11	72.51	104.40	141.67	154.54	160.01
Q12	65.06	92.61	124.37	123.04	130.28

Table 4: DTL quadrupole triplet current setpoints for A/q = 6, computed using Eq. 1 with numbers from Table 1. **Note: The above currents arise from a 105 MHz DTL-LANA simulation.**

5 Stable Beam Tests

Stable beam shifts allocated to HLA development were partially devoted to testing the DTL quadrupole currents in Table 4. Specifically, the goal was to verify that the quadrupole BI relation presented in this note produced a working accelerator tune, with good transmission, at the energies specified in the table, each of which corresponds to the output energy of the DTL tanks.

5.1 Reference RIB Operations Tune

Prior to the August 6th test detailed herein, the DTL was delivering $^{12}Be^{2+}$ (A/q=6) to the DSL experiment in SEBT1, meaning the DTL was injecting 1.5 MeV/u RIB into the superconducting linac. As the DTL had already been tuned by RIB Operations around July 29th, 2019, it was decided to use the existing operations tune as a baseline for comparison with the numbers of Table 4. The recorded operations DTL triplet setpoints and readbacks are shown in Figure 5. These numbers find their origin in the aforementioned averaged operations tune numbers, used for the A/q=6 setup, which are featured on the tuneX-HLA at the time of writing the present report.

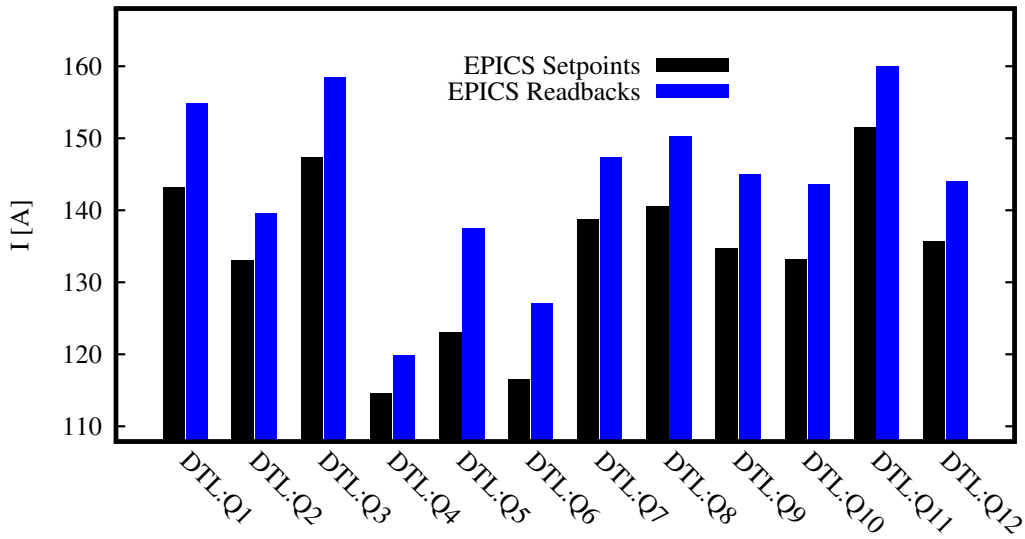

Figure 5: $^{12}Be^{2+}$ 1.5 MeV/u RIB Operations DTL tune, in effect immediately prior to stable beam tests. The EPICS quadrupole setpoints are shown in black and the EPICS readbacks are shown in blue.

Of immediate significance in Figure 5 is the significant disagreement between the quadrupole current setpoints and readbacks in the EPICS control system, with errors on the order of 10A for most quadrupoles. The relative errors between the EPICS setpoitns and the pseudoLangevin currents, in addition to that between the EPICS readbacks and the pseudoLangevin numbers, are shown in Figure 6. Inspection of the former reveals that the first quadrupole triplet was tuned with a significant disagreement for both setpoints and readbacks, with respect to the design tune numbers of Table 4.

Finding 1: The EPICS setpoints for all DTL triplet quadrupoles significantly disagree with their respective readbacks, by up to 10%

Interestingly, again looking at Figure 6, for DTL quadrupole 4 and beyond, the EPICS readbacks systematically display greater agreement with the numbers of Table 4. The DTL tune shown in Figs. 5 and 6 is quoted in the RIB Operations e-log as producing a stable pilot beam ($^{12}C^{2+}$, A/q=6) transmission[1] of 86.8%.

[1] See RIB-Ops e-log entry made on 2019-07-30, 23:22:33, prior to insertion of HEBT stripping foil beyond the DTL.

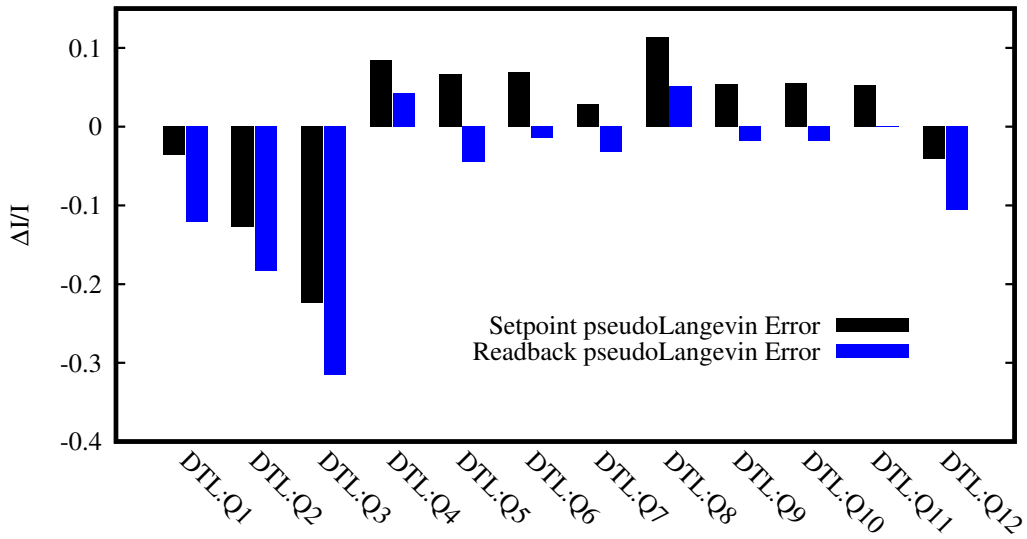

Figure 6: $^{12}Be^{2}+$ 1.5 MeV/u RIB Operations DTL tune, showing relative error between the EPICS setpoitns and the pseudoLangevin currents (black) and the relative error between the EPICS readbacks and the pseudoLangevin currents (blue).

While not presently possible to numerically verify, due to the current lack of a reliable model representing the as-built 106.08 MHz design, the first triplet error pattern may arise from the tuning methodology used by operations, who are known to re-tune tank and buncher phases and amplitudes for maximum linac transmission. Further, the significant setpoint and readback disagreement provided a strong hint that it was entirely possible that loading the DTL quadrupole numbers featured in the operations spreadsheet may not produce the requisite pole-tip fields at all, due to the significance of the discrepancy between both setpoints and readbacks.

5.2 pseudoLangevin DTL Tunes

With the operations DTL tune documented and saved, the next test consisted of loading the pseodoLangevin currents of Table 4 for each of the output DTL energies listed in the table, corresponding to each tank's design output energy. As part of the test, each DTL cavity was phased on the 90° HEBT1:MB0 (Prague) analyzing magnet, with the DTL triplets set to the values of Table 4. Initially, the EPICS setpoints were set to the pseudoLangevin values, which produced no measurable DTL transmission.

Finding 2: The ISAC-DTL triplet quadrupoles, when set to the theoretical currents computed from the original magnetic field surveys (Table 4), performed in 2000, do not produce functioning DTL tunes, resulting in low or no observable beam transmission.

As a follow up to the above tests, the DTL quadrupoles were then set to produce an EPICS readback equal to the pseudoLangevin values of Table 4. The resulting DTL beam transmissions are shown in Figure 7. Each tank was set to the respective quoted design energy, with DTL quadrupole EPICS setpoints manually tuned with a precision of 0.25 A, aiming to equate the EPICS readback value to that of the predicted pseudoLangevin quadrupole numbers. For each tank setup, corresponding to the quoted design energies in Table 4, the relative percent error between the achieved EPICS readback and the predicted currents are shown in Figure 8.

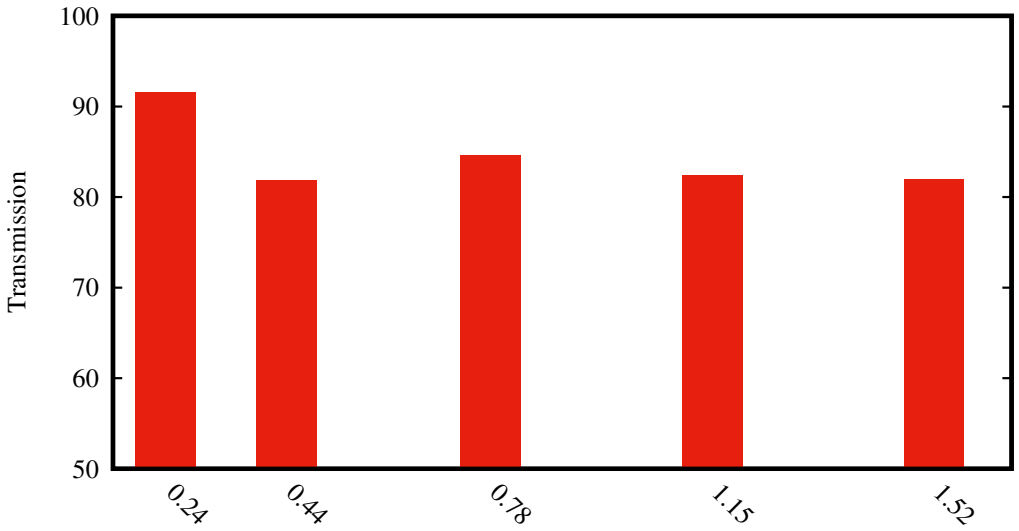

Figure 7: Observed DTL transmissiosn at different output energies, corresponding to each accelerating tank's output design energy. The x-axis is energy in MeV/u. Observe: Tank1 transmission is higher due to a procedural error, and is excluded from consideration as a result.

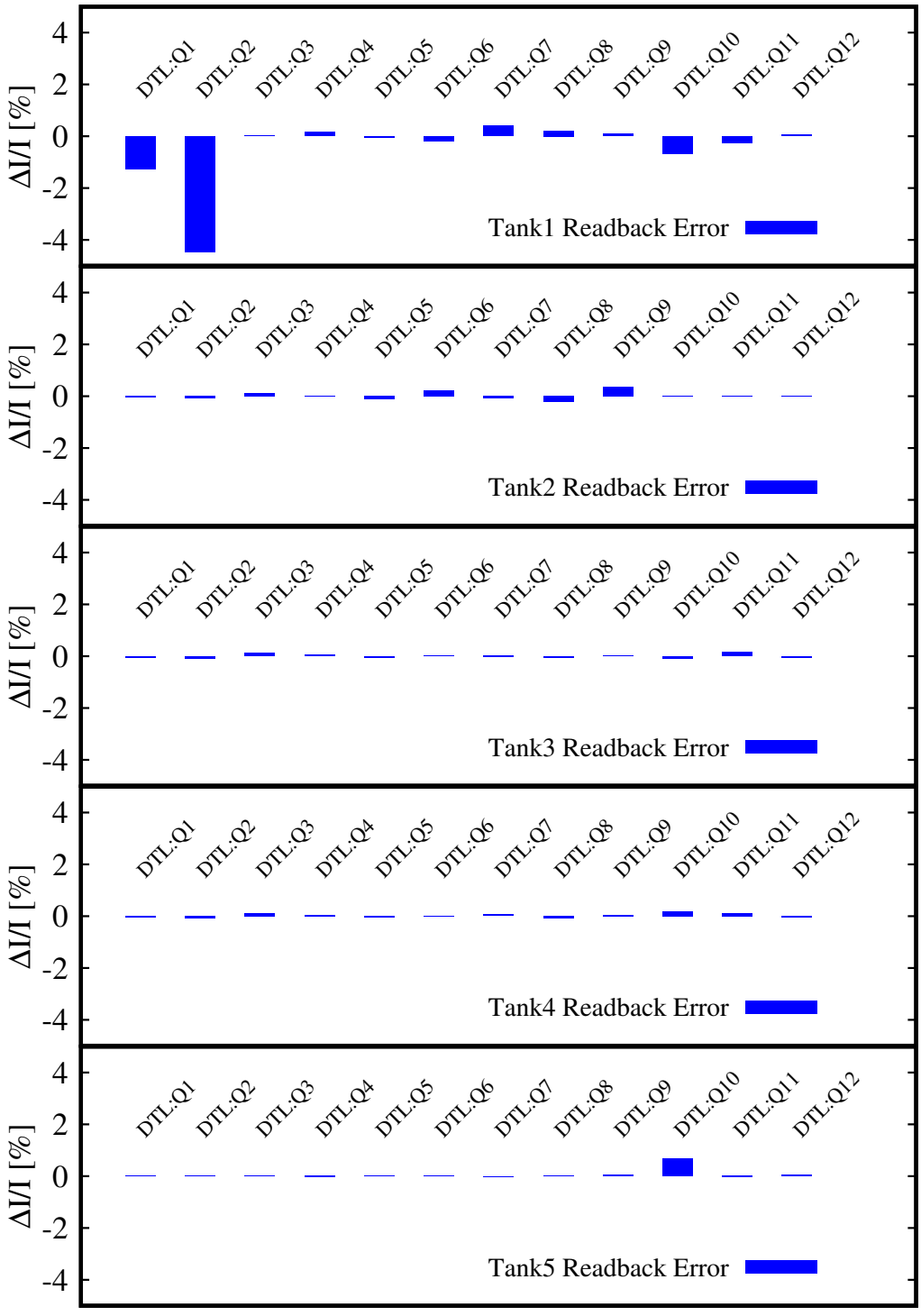

Figure 8: Relative percent errors, for each DTL design energy as tuned during the August 6th 2019 beam tests, corresponding to the quoted tank design energies, with respect to the predicted pseudoLangevin currents of Table 4. A $^{12}C^{2+}$ (A/q=6) beam was used.

An immediate issue must be addressed regarding the 0.238MeV/u measurement for Tank1. Post run data analysis reveals a sizeable error in DTL quadrupoles 1 and 2. This is likely a procedural error on the part of the author, who erroneously set the first two quadrupoles to slightly off nominal values during tank1 setup. Interestingly, when looking at Figure 7, the tank1 energy tune does have a slightly higher transmission than the remainder of the measured energies. As such, the 0.238 MeV/u tank1 DTL tune is excluded from the remainder of the discussion and will necessitate further testing.

Finding 3: Setting the EPICS readbacks to match current values from Table 4 for all DTL quadrupoles produces transmissions in the lower-80% range.

Suspecting the setpoint-readback discrepancy as a cause, the quadrupole currents were then measured with a current meter.

Finding 4: Manually measured DTL quadrupole currents agree with the EPICS setpoints, to within 1%.

The above findings suggest that the EPICS setpoint and readback discrepancy is not to blame for DTL transverse tuning issues. Returning to Figure 5, by setting all EPICS readbacks to match the values of Table 4, the consequence is an effective reduction in setpoints, therefore transverse focussing. In particular, this result may suggest that the quoted design tune imposes transverse gradients that are too strong, requiring an overall reduction of transverse corrective focussing. It could also imply steering issues through the DTL triplets.

As a final note regarding the quadrupole pseudoLangevin tests, when considering Figure 7, excluding tank1 (0.238 MeV/u) due to the above noted error, the theoretical quadrupole setpoints produce transmissions in the lower 80% range. Typically, RIB Operations expects transmissions in the mid to high 90% range for radioisotope beam delivery. Transmissions below this threshold are considered unacceptably low. As such, the tunes obtained from reference [1] appear to produce transmissions which would not be acceptable. As has been pointed out, the aforementioned reference was a preliminary beam simulation, prior to DTL commissioning, in which the accelerator was designed at an operating frequency of 105 MHz.

Finding 5: The theoretical transverse design DTL tunes from [1] do not appear to produce sufficiently high DTL transmissions for sanctioned use by operations.

It must be reiterated that the lack of a verified DTL model, as of writing this report, faithfully reproducing the as built, 106.08 MHz accelerator, renders further commentary on the above finding speculative, and as such this issue is reserved for later investigation. Nevertheless, the results and findings in the present section demands a closer investigation of the DTL transverse tune setpoints, which were provided to ISAC Operations circa 2002. In particular, one must ask why these numbers

never worked, generating the necessity to manually tune the triplets, a complex endeavour which ultimately imposed considerable tuning overhead time.

6 Forensics of the Original Triplet Currents

An excel-like spreadsheet had been provided to operators not long after DTL commissioning was completed as previously stated. To understand why the quoted spreadsheet quadrupole currents never produced working tunes, the BI relationship contained in the operations spreadsheet was plotted and compared to the pseudoLangevin currents of Table 4, shown to produce working though not optimal tunes, in the previous section, in addition to the original raw data, scaled by a factor of 2 to represent the pole-tip field. The comparisons are shown in Figures 9 and 10. Inspection of the former reveals a significant difference between the spreadsheet numbers and the survey data.

Finding 6: The DTL triplet BI quadrupole relation, as provided to ISAC Operations in a DTL tuning spreadsheet, does not agree with the original magnet survey data, for all DTL quadrupoles.

Summary comparison of Figures 9 and 10 does reveal a curious trend, in which all outer triplet quadrupole BI values from the DTL Spreadsheet appear to overestimate the resulting magnet pole tip field, while the inner quadrupole spreadsheet BI values underestimate the pole tip value. As part of this investigation, the spreadsheet BI values for Q1-like quadrupoles have been plotted compared to the pseudoLangevin for Q2-type quadrupoles, and vice versa. This is shown in Figure 11.

Finding 7: The original DTL triplet quadrupole BI derived setpoints, as provided to ISAC Operations in a DTL tuning spreadsheet, were inverted, with outer quadrupoles given an inner quadrupole BI, and vice-versa.

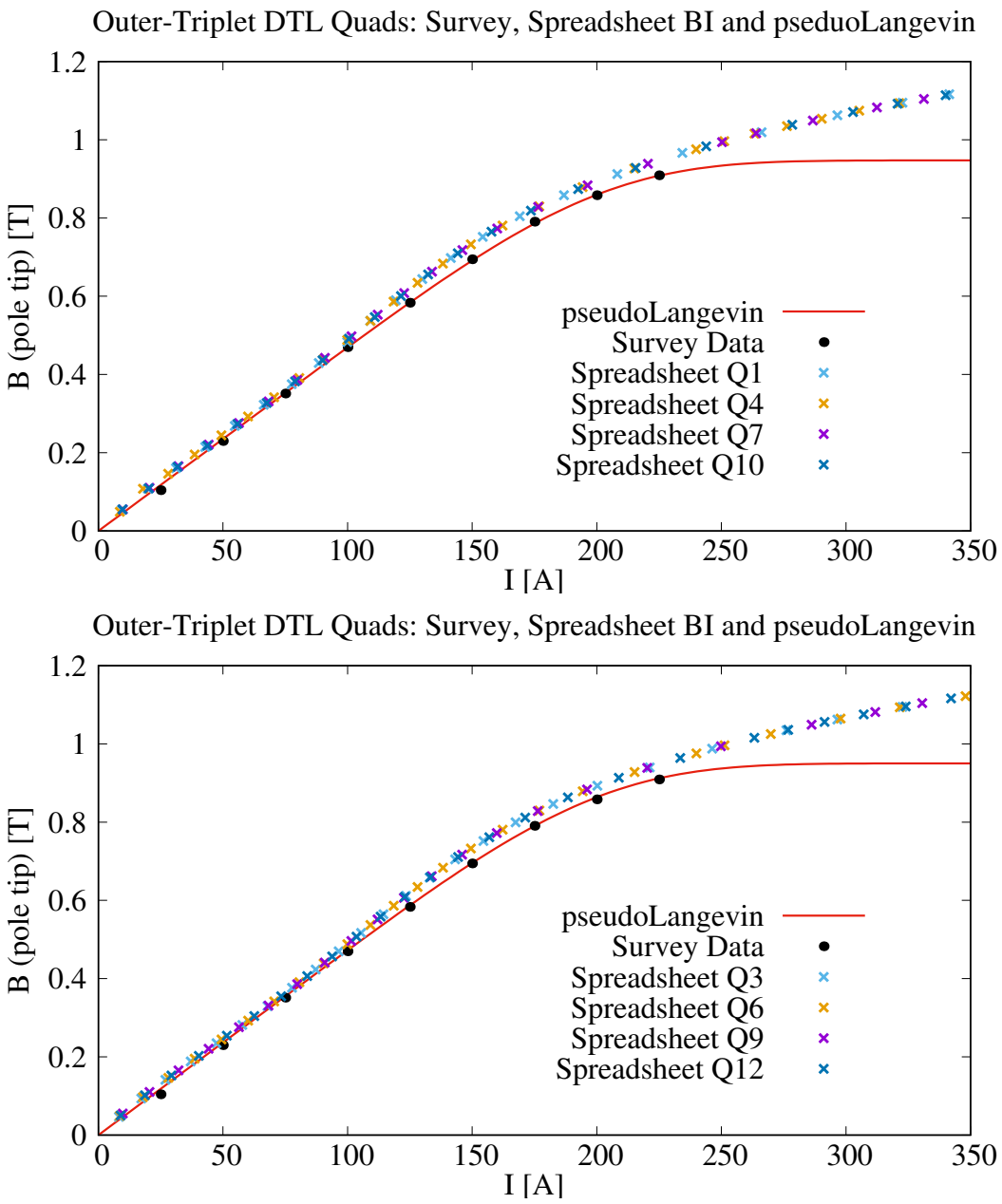

Figure 9: Comparison of the BI relationship from the ISAC Operations DTL spreadsheet for DTL triplet quadrupoles Q1,4,7 and Q10, shown at the top, the first quadrupoles for each of the 4 DTL triplets. DTL triplet quads Q3,6,9 and 12, the last quadrupoles for each triplet are shown at the bottom. For both plots, the pseudoLangevin curve is shown in red, the original survey data as black points, while the original spreadsheet data is plotted as crosses for each quadrupole. X-axis extended to 350 A to show saturatory behavior.

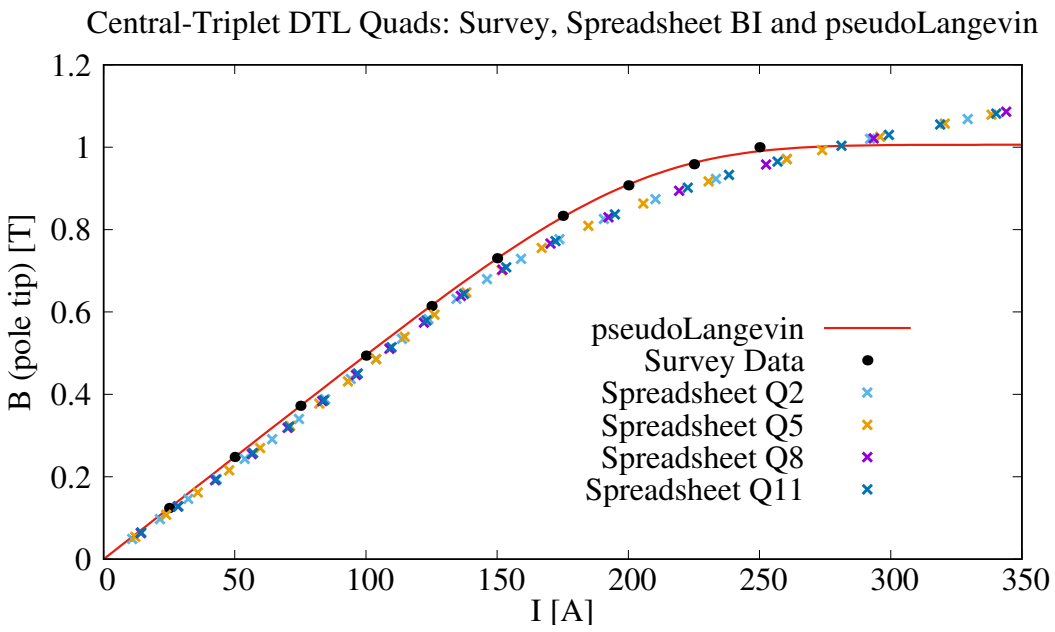

Figure 10: Comparison of the BI relationship from the ISAC Operations DTL spreadsheet for DTL triplet quadrupoles Q2,5,8 and Q11, the central quadrupoles for each of the 4 DTL triplets. The pseudoLangevin curve is shown in red, the original survey data as black points, while the original spreadsheet data is plotted as crosses for each quadrupole. X-axis extended to 350 A to show saturatory behavior.

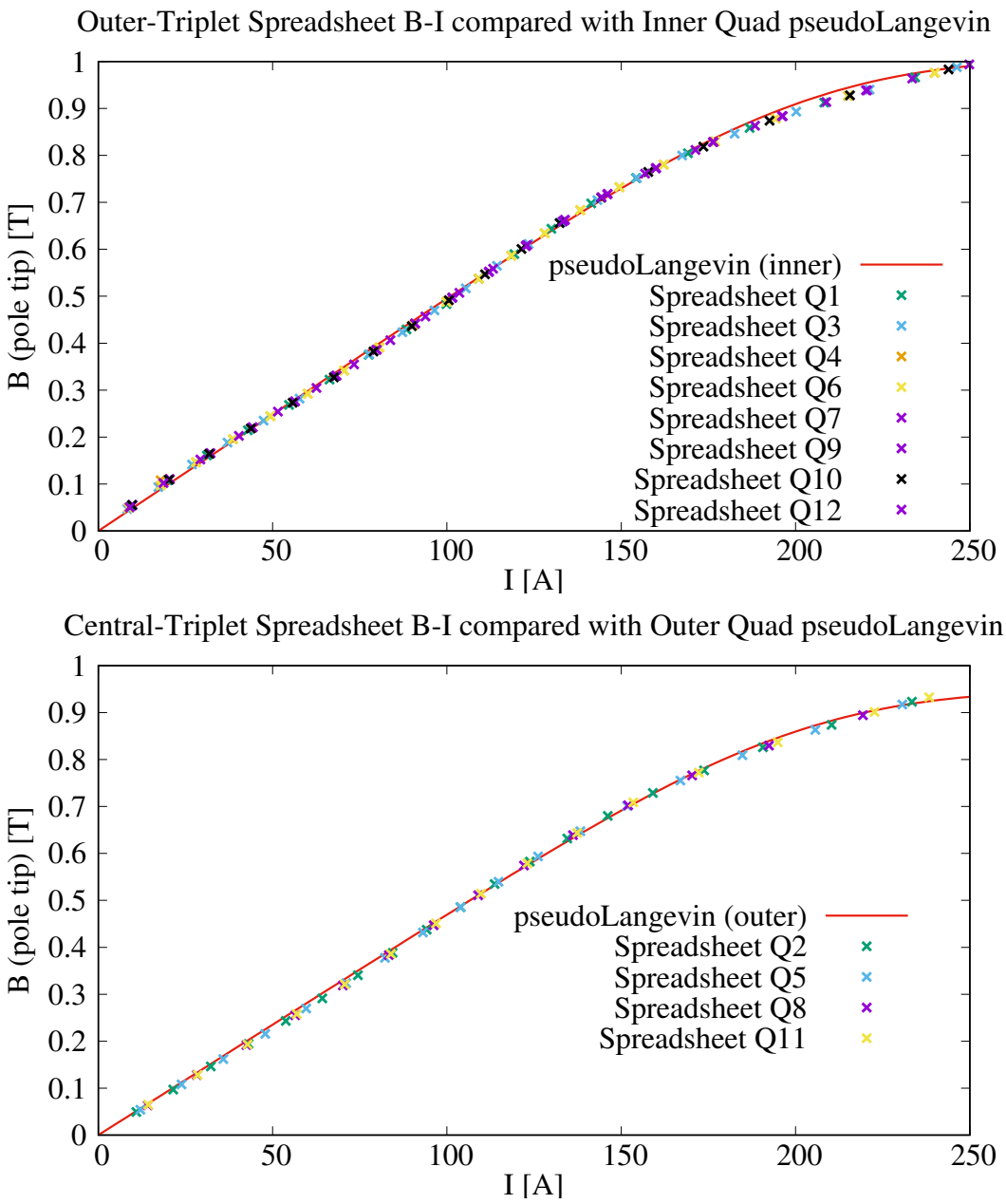

Figure 11: Cross-comparison between spreadsheet outer quadrupole BI values with inner quadrupole pseudoLangevin fit (top), cross-comparison betwen spreadsheet inner quadrupole BI values with outer quadrupole pseudoLangevin fit (bottom).

7 Shifting Focus to the MEBT Section

The above findings have not produced strong evidence for abnormal behavior on the part of the DTL triplets. While more detailed analysis of the devices could be carried out, it is worth noting that the RIB Operations values for the triplets, while off-nominal in terms of predicted currents, do produce high transmissions across the accelerator. Moreover, the high degree of reproducibility observed by operators when loading saved triplet setpoints, implies that the devices appear to be operating nominally. As such, the present investigation shifts its focus to the injection and matching into the DTL.

The medium energy beam transport (MEBT) line, joining the RFQ to the DTL, consists of 13 Danfysik L1 type quadrupoles, with a measured effective length of 182.0 mm. The first five quadrupoles are tilted on a 45° slant, matching the local vertical and horizontal axis definitions of the RFQ vanes, themselves tilted by 45°. Between MEBT quadrupoles 5 and 6, the beamline optical elements are rotated back to their nominal orientation, by 45°, after which the horizontal axis is parallel to the floor and vertical axis perpendicular. The MEBT design tune produces a double waist after MEBT:Q5, coinciding with the location of an optional stripping foil. Further, a 106.08 MHz bunch rotator cavity further provides a longitudinal time focus at the same location.

Measurements performed by Doug Preddy, from the TRIUMF Beamlines Group, revealed that all MEBT quadrupoles were level and free from pitch and roll errors, to within $\pm$ 0.1°, which was noted as a typical tolerance found across the TRIUMF site, ruling out the possibility of quadrupole misalignment.

Finding 8: The MEBT quadrupoles are free from pitch or roll misalignments, to within $\pm$0.1°.

It was further noted that the magnetic steerers used in the MEBT section are known to be insensitive to vertical misalignments on the order of a degree or so. As such, this rules out optical misalignments as a main contributing factor to explain the anomalous DTL transverse tune.

During investigation of the beamline, it was observed by the author that a sizeable crack in the floor of the ISAC experimental hall floor had developed in what was originally a concrete floor joint, shown in Figure 12, at the top. This crack had grown to sufficient dimensions that water inflitration had presumably become a concern, as caulking had been injected along its entire length, shown at the bottom of Figure 12. The crack itself was found to have produced a level offset in the ISAC experimental hall floor, with the RFQ side being lower than the remainder of the ISAC Experimental Hall floor, by roughly half to three quarters of a centimeter. While this crack does not appear to have affected the MEBT line in terms of angular misalignments, a closer look was given to the RFQ itself. Figure 14 shows a closeup of the bellows joint linking the RFQ to the MEBT section. It was observed that the guide screw joining both sides of the joint had a visible tilt on it, hinting at a possible misalignment.

Figure 12: Top: Crack in the ISAC Experimental Hall floor, running parallel to the RFQ. The crack developed in what was originally a concrete floor joint. Bottom: close up of the crack, showing its extent and presence of weathered caulking.

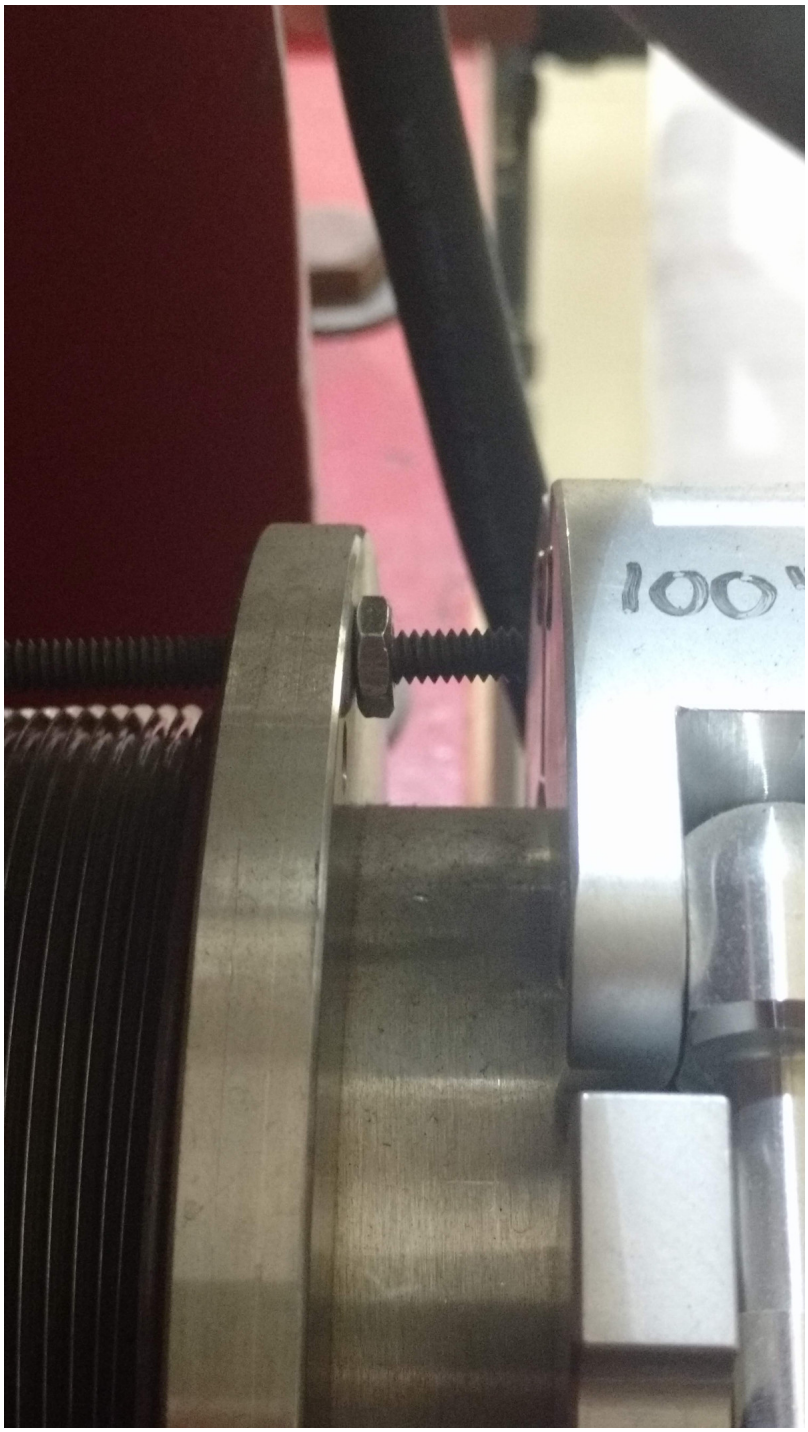

Figure 13: ISAC RFQ to MEBT line bellows joint, showing crooked guide screw.

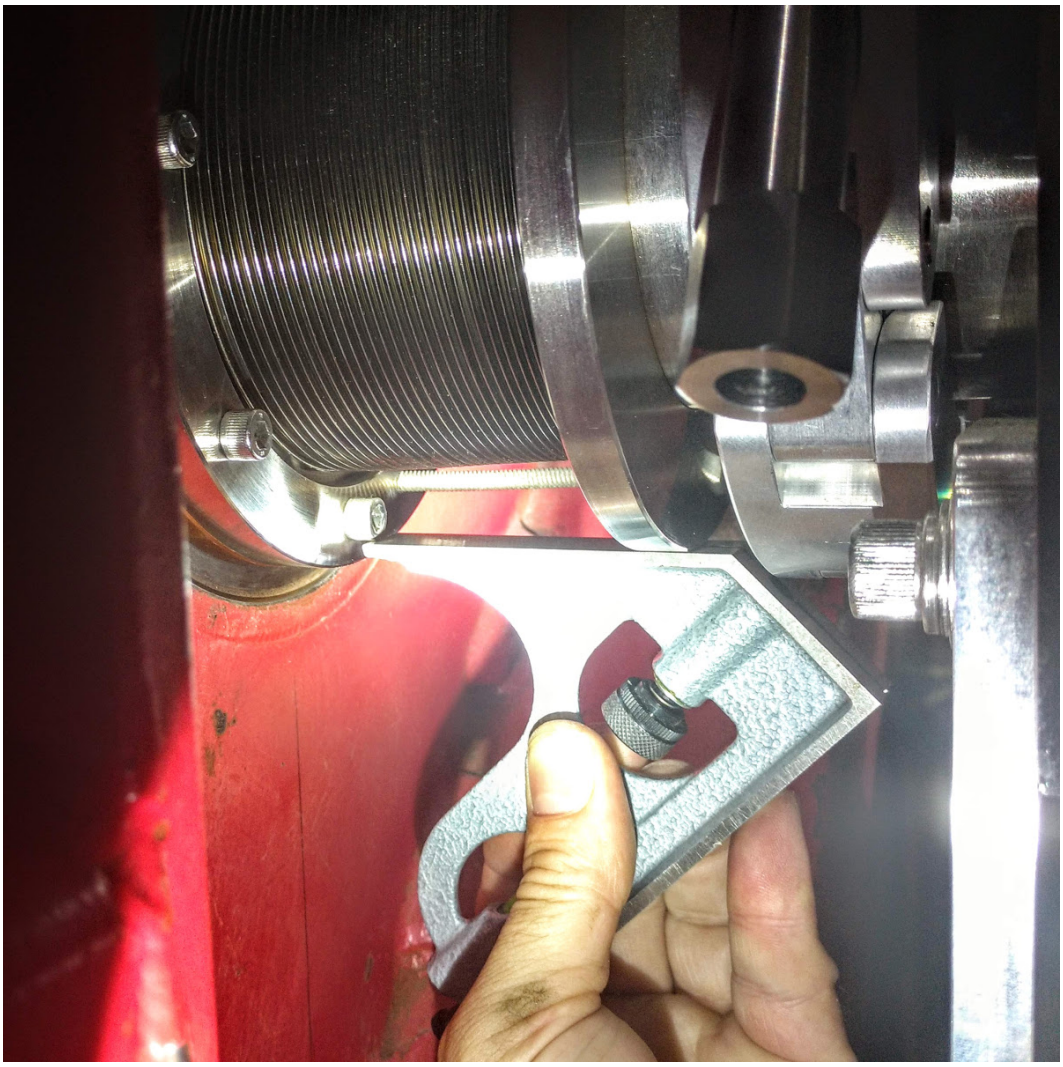

Figure 14: ISAC RFQ to MEBT line bellows joint misalignment. The straightedge has been placed flush below the MEBT side of the Bellows joint, highlighting the offset between both sides.

Finding 9: The ISAC RFQ to MEBT Bellows joint appears to be misaligned.

While the above demonstrates an externally measurable misalignment between the RFQ and the MEBT line, this cannot be extrapolated to imply a misalignment of the actual optical elements themselves. In particular, no specific alignment tolerance between the RFQ vanes, the Bellows joint and the MEBT line optical axis can be guaranteed. Instead, with the above evidence at hand, an analysis of the ISAC tunes through the MEBT section was carried out. A bash script was written to parse through all saved RIB Operations tunes, dating back to 2000, the initial operation of the ISAC-I accelerator. The saved element setpoints of the MEBT optics were extracted. No particular

trends were identified looking at the MEBT quadrupoles, which are therefore excluded from the present discussion.

Prior to figure interpretation, a short word regarding the significance of the extracted savetune data is in order. Operators in the RIB control room routinely save tunes during the process of setting up accelerators, or following any corrective action, for example on-line tune adjustment. Savetunes do not necessarily reflect a finished and working tune, form source to experiment. Rather, the save tune utility allows operators to save the present tune state, allowing restoration of the values at an arbitrary time, for an arbitrary reason.

As such, parsing through all tune files will produce all saved working and final tunes, but it will also present all other intermediate states, which are not guaranteed to be proper working tunes. Nevertheless, by extracting all these numbers, it is hoped to gain insight into the corrective steering of the MEBT section, for a period spanning 19 years. Finally, varying A/q's will necessitate varying steering. No A/q filtering was applied, instead all raw tunes, independent of A/q are displayed. All tunes in the MEBT section feature a beam energy of 0.153 MeV/u, the RFQ output energy.

First, the x-steering in the MEBT section is presented in Figure 15. The overall observable x-steering trend is relatively neutral, with steerers XCB1, XCB5 and XCB12 almost never saved with off zero values. Steerers XCB3 and XCB9 do display variability, with XCB9 trending toward neutral while XCB3 displays an increasing corrective steering trend up to the present.

The steering excursions are more striking when looking at the extracted corrective Y-steering, shown in Figure 16. For y-steerers YCB3, 7A and 7B, a significant and sustained trend can be seen up to the present day. It is useful to remember that, steerers X/YCB3 and X/YCB5 are actually on a 45° tilt with respect to the floor, due to the RFQ's orientation.

The combination of slight x-steering (XCB3) and considerable y-steering (YCB3,7A,7B) provides clear evidence of an optical axis misalignment between the RFQ, the MEBT section and the DTL.

Finding 10: Corrective MEBT steering, particularly y-steering, has been increasing since initial accelerator commissioning.

As a test of the RFQ-MEBT alignment, output RFQ beam of $^{38}Ar^{7+}$ (A/q = 5.429) was taken to MEBT:RPM5, the rotary position monitor at the approximate location of the design MEBT double transverse waist. The test involved removing all corrective steering between the RFQ and MEBT:RPM5, to look at the resulting centroid offsets for both x- and y- dimensions. The test was performed after the beam delivery group had tuned the section up to HEBT2/DRAGON, following standard procedures. This namely involved the use of corrective x- and y- steering in the MEBT section, loaded from previous operational tunes, using the standard operations procedure, also featuring the off-theory DTL triplet currents for experiment delivery.

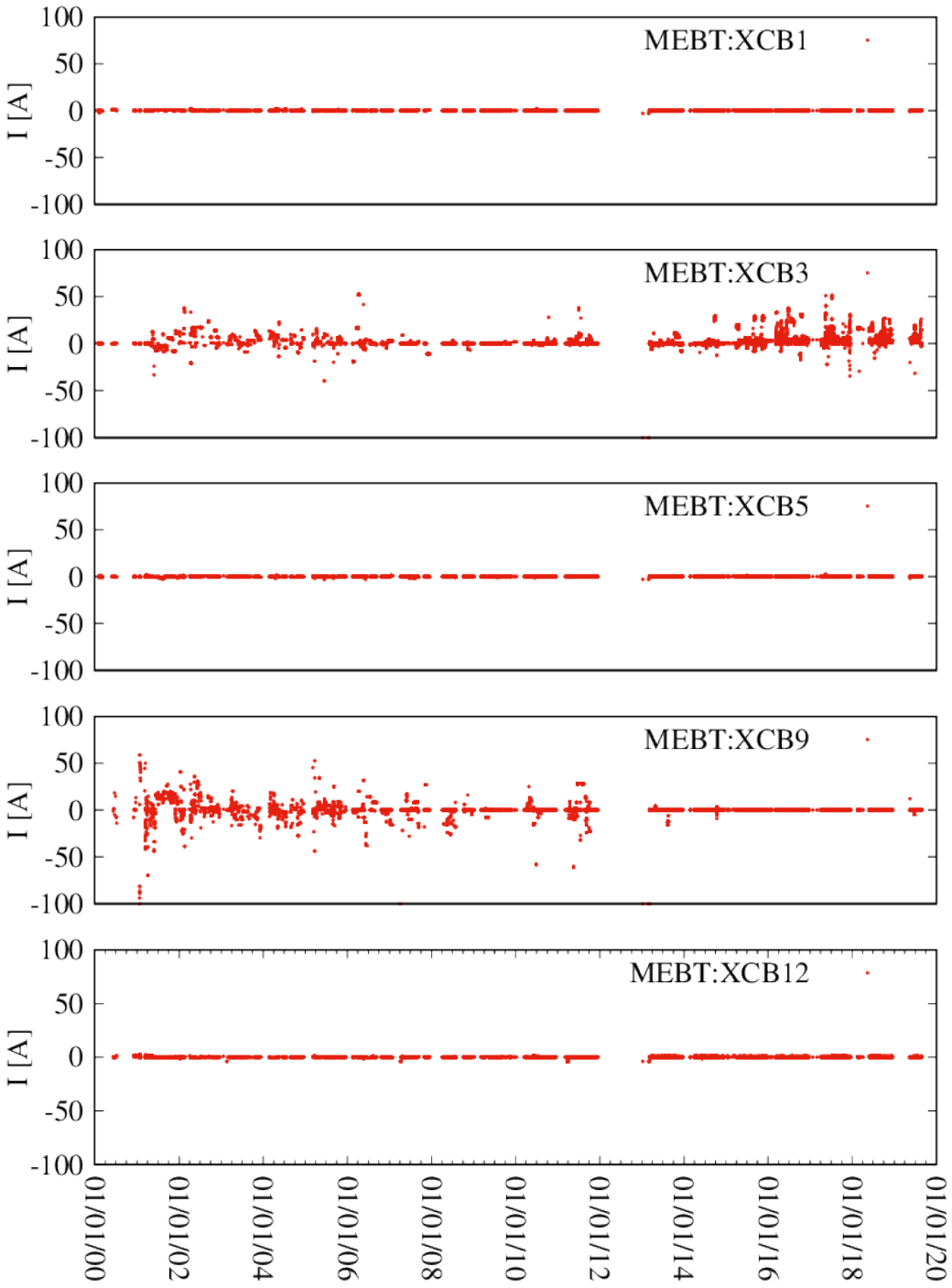

Figure 15: RIB Operations savetune extracted x-steering values, dating back to 2000.

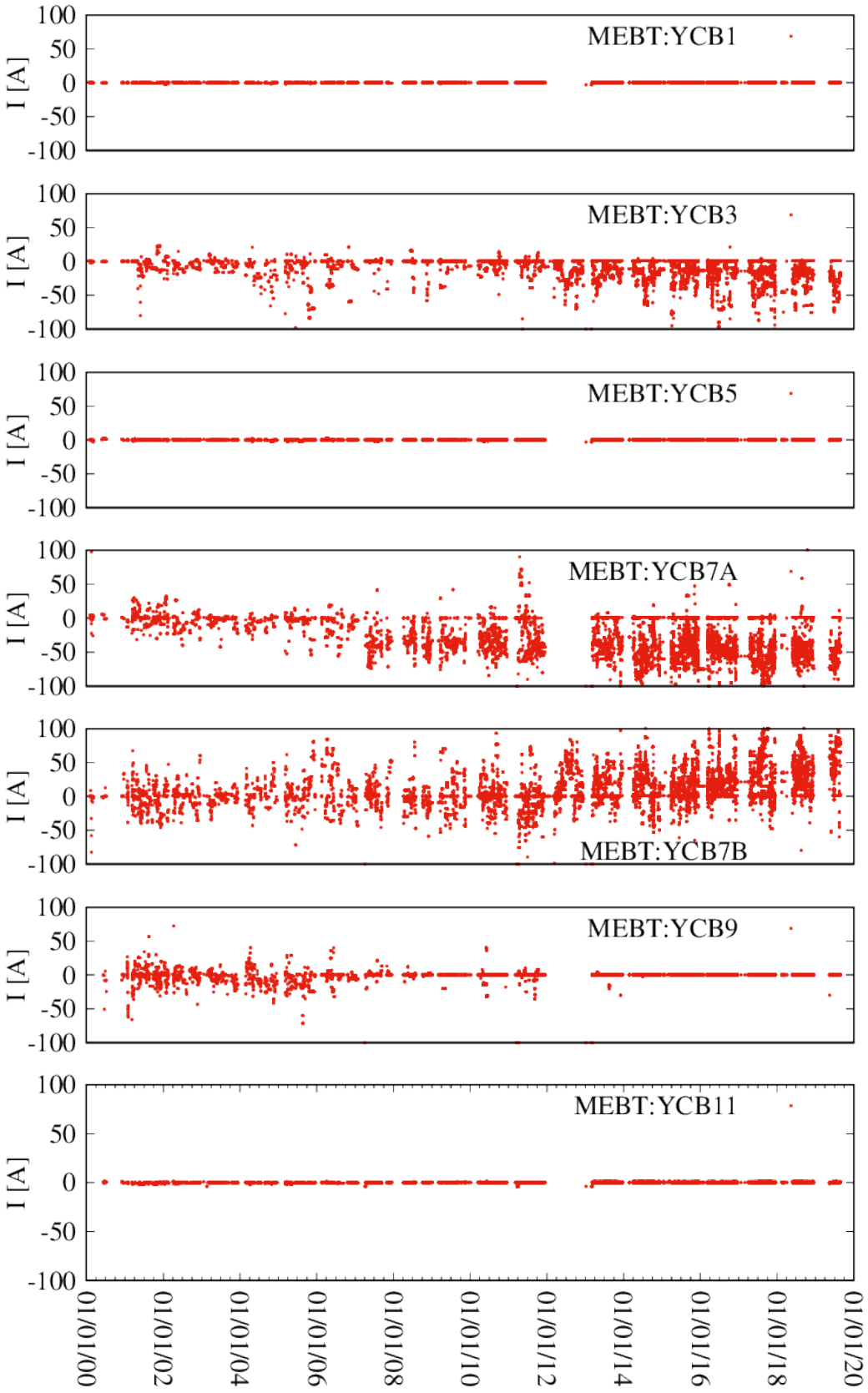

Figure 16: RIB Operations savetune extracted y-steering values, dating back to 2000.

Figure 17 shows beam on MEBT:RPM5, with and without corrective steering in both transverse dimensions. Blue traces denote the original tune featuring corrective steering, as established by the Beam Delivery group. The steered beam profiles are centered on the beam optical axis, at least at the location of the RPM. The red trace shows beam position on the RPM when all steering is removed. The centroid differences are of roughly 0.12 cm for x and 0.3 cm for y. While it is possible that off-center beam exiting the RFQ receives additional steering from the first five MEBT quadrupoles, due to traversing their magnetic field off-axis, the offsets shown in Figure 17 do nevertheless provide further evidence supporting an RFQ-MEBT misalignment.

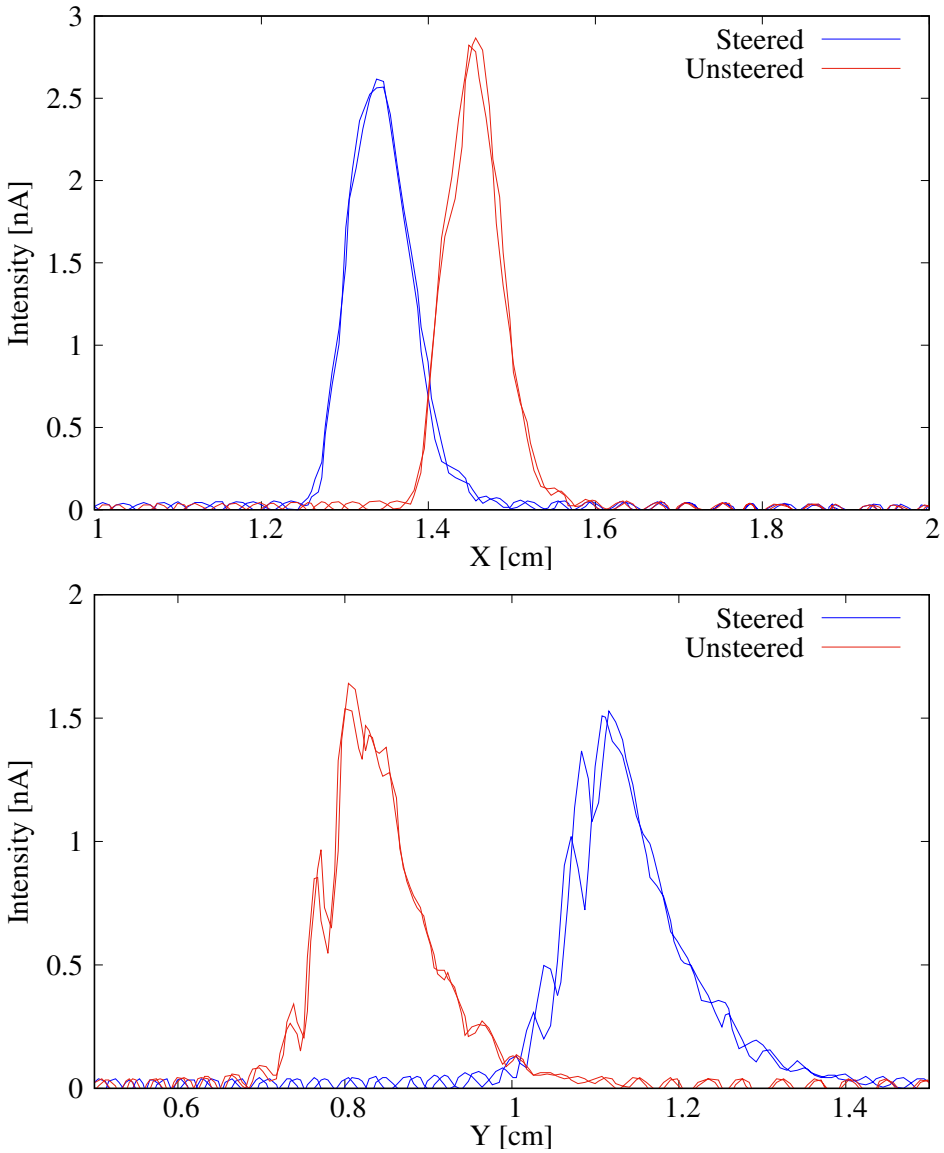

Figure 17: Top: X-traces measured on MEBT:RPM5. Bottom: Y-traces measured on MEBT:RPM5. The traces show the effect of corrective steering on output RFQ beam in the local x- and y-dimensions. $38Ar^{7+}$ beam (A/q = 5.429) used for the measurement, at E = 0.153 MeV/u. X-axis dimensions denote the raw RPM readback in both figures.

8 DTL Theory pseudoLangevin Tune

The same $38Ar^{7+}$ beam was then tuned through the DTL at an output energy corresponding to Tank2 output. The pseudoLangevin theory currents from Table 4 were loaded, corresponding to Tank2 computed numbers. Initially, poor transmission was observed, in the upper 70% range. Typically, at this point, RIB Operations or Beam Delivery would tune the DTL triplet quadrupoles, looking at transmission through the DTL, a procedure which typically allows the attainment of transmissions in the mid 90% range, suitable for experiment delivery.

Knowing that there is a likely misalignment, mainly in the vertical dimension, the DTL quads were left at theory, and additional y-steering in MEBT was provided using MEBT:XCB9 and XCB11, while the x-steering was adjusted with the MEBT dipole magnets (MB1 and MB2). Without touching the triplets, which remained at theory, a beam transmission of 98.0% was attained.

Finding 11: The theoretical DTL Triplet Quadrupole currents listed in Table 4 produce high transmission tunes when appropriate corrective MEBT steering, particularly in the y-dimension, is used.

The coupling of findings 2 and 11 strongly suggest that the triplet quadrupole currents used by Operations and Beam Delivery not only produce corrective focussing, but likely produce corrective steering as well. The initial loading of theory currents without additional corrective y-steering, discussed in Section 5.2, supports this hypothesis.

9 Conclusion

The work done in this report was originally motivated by the observation by RIB Operations that the transverse DTL quadrupole currents did not appear to work, requiring significant retuning. An investigation of the BI characterization of the ISAC Drift Tube Linac triplet quadrupoles, using an empirical hyperbolic pseudoLangevin function, was performed. Original magnet survey data, performed during the course of the year 2000, have been reanalyzed and fit to the aforementioned function. The fits show strong agreement with the original survey data, with residual errors on the order of 2-3%. These fits were then used to compute a set of triplet currents for the DTL, corresponding to the original transverse design tune, dating back to 1999.

The DTL was initially re-tuned with these re-computed numbers, which were found to produce low- or no- transmission across the accelerator, at its different design energies. A significant discrepancy between EPICS setpoint and readback was identified, with readbacks being systematically higher than setpoints. However, current measurements of the DTL quadrupoles, showing agreement between EPICS setpoints and measured currents to within 1%, have ruled this out as a cause.

Further investigation into the original quadrupole current values, provided to ISAC/RIB Operations in the form of a spreadsheet, originating no later than 2002, has revealed an error in the processing of DTL BI data, in which the characterizations were erroneously inverted between outer and inner type quadrupoles. While the former likely contributed to the persistent transverse DTL tuning diffi-

culties, the present investigation has demonstrated that it is not the sole cause. Simply setting the DTL transverse optics to the corrected numbers did not produce satisfactory transmission.

An inspection of the ISAC-I accelerator has revealed strong evidence of a misalignment between the RFQ and the MEBT line, requiring significant corrective steering. This steering has been observed to increase over the last years, via parsing of RIB Operations tunes and can potentially be explained by the ISAC Experimental Hall floor under the RFQ and MEBT line settling. This hypothesis is further supported by the observation of significant cracks in the floor, a misaligned Bellows between the RFQ and MEBT, in addition to beam-based measurements. The MEBT quads were found to be free of pitch or roll misalignments, to within $\pm 0.1^{\circ}$, noted to be a typical value on site by the Beamlines group.

Following this observation, the pseudoLangevin computed DTL triplet currents were again loaded, for an energy corresponding to Tank2 output with a $38Ar^{7+}$ beam. Unlike the first attempt with an A/q = 6, the second attempt involved the addition of corrective y-steering in the MEBT section, specifically using MEBT:YCB9 and MEBT:YCB11. The pseudoLangevin quadrupole setpoints produced a 98% DTL transmission, demonstrating their viability and implying nominal DTL triplet quadrupole behavior, when compared to their original field surveys.

Finally, since the present work was aimed at verifying the transverse DTL tune when compared to initial modelling, the scope and depth of the alignment issues in the MEBT section were only presented to a degree relevant to the stated goal. As such, the present report further concludes that a more thorough investigation of the overall alignment state of the ISAC-I heavy ion accelerator, together with its MEBT section, to be of high importance for the near to medium term future.

Acknowledgements

Thanks to Bob Laxdal, who tirelessly searched for original materials and information on the ISAC DTL, used in the present work. Gratitude is expressed to the members of RIB Operations for their candor and assistance. Sincere gratitude to Spencer Kiy for useful discussions and help coordinating beamtime for this investigation. Thanks to Matt Pearson for assisting in measuring the RFQ Bellows offset.

This note was modified on 2021-02-05 with the addition of Appendix D, which displays raw DTL triplet magnetic field surveys. These were used to compute the Wollnik integrals of the quadrupoles, allowing for a parametrization of their fringe fields. In addition, their effective lengths are measured.

Appendices

A Original Triplet BI Survey Data

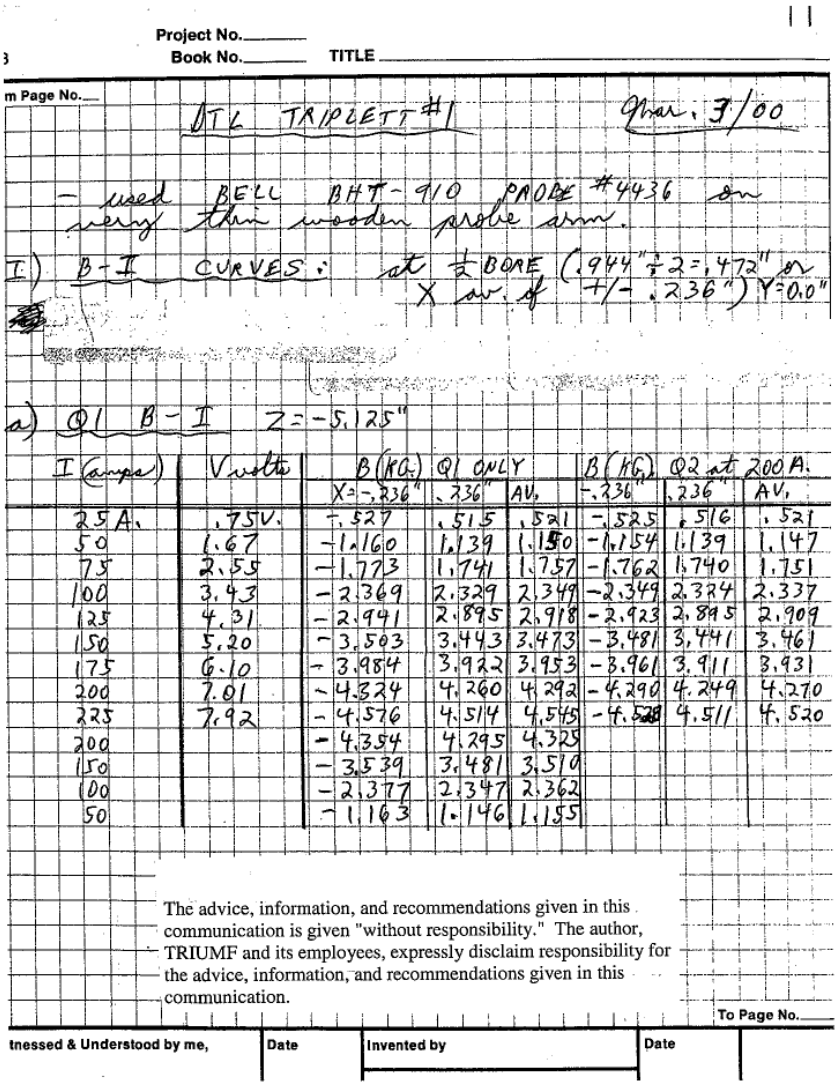

Project No.
Book No. TITLE

m Page No.

DTL TRIPLETT #1 Mar. 7/00

- used BELL BHT-910 PROBE #4436 on very thin wooden probe arm.

I) B-I CURVES: at ½ BORE (.944" ÷ 2 = .472" on X av. of +/- .236") Y=0.0"

a) Q1 B-I Z=-5.125"

I (amps)	V volts	B (KG) X=-.236"	Q1 ONLY .236"	AV.	B (KG) -.236"	Q2 at 200A. .236"	AV.
25A.	.75V.	-.527	.515	.521	-.525	.516	.521
50	1.67	-1.160	1.139	1.150	-1.154	1.139	1.147
75	2.55	-1.773	1.741	1.757	-1.762	1.740	1.751
100	3.43	-2.369	2.329	2.349	-2.349	2.324	2.337
125	4.31	-2.941	2.895	2.918	-2.923	2.895	2.909
150	5.20	-3.503	3.443	3.473	-3.481	3.441	3.461
175	6.10	-3.984	3.922	3.953	-3.961	3.911	3.931
200	7.01	-4.324	4.260	4.292	-4.290	4.249	4.270
225	7.92	-4.576	4.514	4.545	-4.528	4.511	4.520
200		-4.354	4.295	4.325			
150		-3.539	3.481	3.510			
100		-2.377	2.347	2.362			
50		-1.163	1.146	1.155			

To Page No.

tnessed & Understood by me, Date Invented by Date

From Page No.

b) Q3 B-I (Z = 5.125" Y = 0.0")

I (amps)	V (volts)	B (KG.) Q3 ONLY X = -.236"	.236"	AV.	B (KG.) Q2 at 200 A. -.236"	.236"	AV.
25 A	.75 V.	-.534	.513	.523	-.528	.518	.523
50 A.	1.66	-1.175	1.136	1.155	-1.167	1.146	1.157
75	2.54	-1.793	1.730	1.761	-1.781	1.755	1.768
100	3.42	-2.398	2.319	2.358	-2.373	2.346	2.360
125	4.29	-2.987	2.887	2.937	-2.950	2.919	2.935
150	5.18	-3.546	3.432	3.489	-3.502	3.469	3.486
175	6.07	-4.032	3.904	3.968	-3.997	3.940	3.964
200	6.97	-4.384	4.229	4.307	-4.330	4.266	4.298
225	7.88	-4.633	4.476	4.555	-4.584	4.518	4.551
200		-4.404	4.265	4.335			
150		-3.572	3.470	3.521			
100		-2.414	2.338	2.376			
50		-1.178	1.144	1.161			

c) Q2 B-I (Z = 0.0", Y = 0.0")

I (amps)	V (volts)	B (KG.) Q2 ONLY X = -.236"	.236"	AV.	B (KG.) Q1/Q3 at 178A. -.236"	.236"	AV.
25A	1.12 V.	.620	-.624	.622	.604	.641	.623
50	2.24	1.240	-1.240	1.240	+1.202	-1.283	1.242
75	3.36	1.858	-1.863	1.861	1.803	-1.911	1.857
100	4.50	2.475	-2.464	2.470	2.473	-2.464	2.469
125	5.64	3.073	-3.071	3.072	3.081	-3.066	3.074
150	6.80	3.658	-3.646	3.652	3.659	-3.649	3.654
175	7.98	4.175	-4.156	4.166	4.174	-4.145	4.160
200	9.18	4.540	-4.533	4.537	4.503	-4.480	4.492
225	10.39	4.801	-4.786	4.794	4.770	-4.749	4.760
250	11.64	5.008	-4.989	4.999	4.944	-4.958	4.976
200		4.557	-4.548	4.553			
150		3.708	-3.696	3.702			
100		2.510	-2.506	2.508			
50		1.269	-1.268	1.269			

To Page No.

Witnessed & Understood by me, Date | Invented by Date | Recorded by

From Page No.

DTL TRIPLETT #2 July 5/2000

- used BELL BHT-910 PROBE # 4436 on very thin wooden probe arm.

I) B-I Curves: at 1/2 BORE (.944" ÷ 2 = .472" dia., Y=0.0" or X dir. of +/- .236")

a) Q1 B-I Z = -5.125"

I amps	V volts	B(KG.) Q1 ONLY X=-.236"	.236"	AV.	B(KG.) Q2 at 200A -.236"	.236"	AV.
25A.	.79V.	-.538	.547	.540	-.543	.546	.545
50	1.70	-1.158	1.165	1.162	-1.155	1.168	1.162
75	2.59	-1.761	1.770	1.766	-1.755	1.775	1.765
100	3.48	-2.347	2.356	2.352	-2.336	2.363	2.350
125	4.37	-2.918	2.931	2.925	-2.904	2.948	2.926
150	5.27	-3.472	3.487	3.480	-3.454	3.501	3.478
175	6.18	-3.950	3.970	3.960	-3.921	3.978	3.950
200	7.10	-4.297	4.312	4.305	-4.259	4.322	4.291
225	8.03	-4.550	4.560	4.555	-4.508	4.573	4.541
200		-4.323	4.334	4.329			98.5%
150		-3.503	3.526	3.515			
100		-2.363	2.371	2.367			
50		-1.169	1.175	1.172			

To Page No.

Project No._____
Book No._____ TITLE _____

From Page No.__

b) Q3 B-I (Z = 5.125", Y = 0.0")

I (amps)	V (volts)	B (KG.) Q3 ONLY X = -.236"	.236"	AV.	B (KG.) Q2 at 200A. -.236"	.236"	AV
25A	.81 V.	-.542	.557	.550	-.537	.553	+.54
50	1.70	-1.149	1.186	1.168	-1.148	1.183	1,16
75	2.59	-1.742	1.804	1.773	-1.745	1.799	1.77
100	3.47	-2.324	2.412	2.368	-2.322	2.401	2.36
125	4.36	-2.889	2.999	2.944	-2.886	2.992	2.94
150	5.26	-3.439	3.566	3.502	-3.437	3.560	3.498
175	6.16	-3.915	4.049	3.982	-3.908	4.045	3.985
200	7.08	-4.245	4.394	4.320	-4.243	4.382	4.312
225	8.01	-4.512	4.650	4.581	-4.493	4.640	4.567
200		-4.275	4.420	4.348			
150		-3.473	3.593	3.533			
100		-2.343	2.417	2.380			
50		-1.162	1.190	1.176			

c) Q2 B-I (Z = 0.0", Y = 0.0")

I (amps)	V (volts)	B (KG.) Q2 ONLY X = -.236"	.236"	AV.	B (KG.) Q1/Q3 at 178A. -.236"	.236"	AV.
25 A.	1.13 V.	.620	-.624	.622	.620	-.620	.620
50	2.26	1.238	-1.244	1.241	1.239	-1.239	1.239
75	3.40	1.855	-1.860	1.858	1.857	-1.853	1.855
100	4.55	2.462	-2.468	2.465	2.470	-2.463	2.467
125	5.71	3.066	-3.057	3.062	3.067	-3.058	3.063
150	6.89	3.645	-3.639	3.642	3.648	-3.635	3.642
175	8.09	4.155	-4.146	4.151	4.151	-4.136	4.144
200	9.30	4.518	-4.513	4.516	4.506	-4.503	4.505
225	10.55	4.782	-4.778	4.780	4.783	-4.756	4.770
250	11.82	5.005	-4.993	4.997	4.988	-4.947	4.968
200		4.535	-4.545	4.540			
150		3.697	-3.683	3.690			
100		2.503	-2.498	2.501			
50		1.270	-1.266	1.268			

To Page No.____

tnessed & Understood by me, | Date | Invented by | Date

Recorded by

DTL TRIPLETT #3 Sept. 6/2000

-used BELL BHT-910 probe #4436 on very thin wooden probe arm.

I) B-I Curves: at ± bore (.944" ÷ 2 = .472" dia. or X = ± .236") Y = 0.0"

a) Q1 B-I Z = -5.125"

I (amps)	V volts	B(KG.) Q1 ONLY X = -.236"	B(KG.) Q1 ONLY .236"	B(KG.) Q1 ONLY AV.	B(KG.) Q2 at 200A -.236"	B(KG.) Q2 at 200A .236"	B(KG.) Q2 at 200A AV.
25A	.71V.	-.496	.493	.495	-.515	.515	.515
50	1.62	-1.131	1.131	1.131	-1.137	1.136	1.137
75	2.50	-1.738	1.738	1.738	-1.746	1.746	1.746
100	3.37	-2.322	2.320	2.321	-2.321	2.324	2.323
125	4.24	-2.897	2.896	2.897	-2.902	2.895	2.899
150	5.11	-3.447	3.446	3.447	-3.447	3.451	3.449
175	5.99	-3.941	3.932	3.937	-3.931	3.935	3.937
200	6.89	-4.274	4.267	4.271	-4.267	4.254	4.261
225	7.80	-4.521	4.515	4.518	-4.511	4.500	4.506
200		-4.293	4.299	4.296			99.7%
150		-3.476	3.485	3.481			
100		-2.342	2.345	2.344			
50		-1.149	1.149	1.149			

From Page No.

b) Q3 B-I (Z = 5.125" Y = 0.0")

I (amps)	V (volts)	B (KG.) Q3 ONLY X = -.236"	.236"	AV.	B (KG.) Q2 at 200A -.236"	.236"	AV.
25A.	.74V.	-.500	.516	.508	-.500	.516	.508
50	1.64	-1.113	1.154	1.134	-1.112	1.152	1.132
75	2.52	-1.719	1.783	1.751	-1.718	1.783	1.751
100	3.40	-2.287	2.380	2.333	-2.289	2.377	2.333
125	4.27	-2.846	2.966	2.906	-2.849	2.960	2.905
150	5.15	-3.386	3.530	3.458	-3.383	3.519	3.451
175	6.04	-3.864	4.031	3.948	-3.859	4.017	3.938
200	6.94	-4.179	4.374	4.277	-4.181	4.348	4.265
225	7.86	-4.417	4.630	4.524	-4.422	4.607	4.515
200		-4.204	4.391	4.298			
150		-3.412	3.566	3.489			
100		-2.303	2.401	2.352			
50		-1.131	1.177	1.154			

c) Q2 B-I (Z = 0.0", Y = 0.0")

I (amps)	V (volts)	B (KG.) Q2 ONLY X = -.236"	.236"	AV.	B (KG.) Q1/Q3 at 178A -.236"	.236"	AV.
25A.	1.11	.612	-.621	.617	.612	-.621	.617
50	2.22	1.234	-1.248	1.240	1.226	-1.237	1.232
75	3.33	1.840	-1.855	1.848	1.838	-1.850	1.844
100	4.45	2.446	-2.464	2.454	2.444	-2.460	2.452
125	5.59	3.044	-3.062	3.053	3.046	-3.064	3.055
150	6.74	3.623	-3.647	3.635	3.618	-3.641	3.630
175	7.92	4.126	-4.158	4.142	4.115	-4.145	4.130
200	9.11	4.482	-4.525	4.503	4.470	-4.512	4.491
225	10.33	4.746	-4.790	4.768	4.731	-4.765	4.748
250	11.57	4.946	-5.003	4.974	4.938	-4.969	4.954
200		4.514	-4.546	4.530			
150		3.668	-3.700	3.684			
100		2.481	-2.499	2.490			
50		1.256	-1.270	1.263			

To Page No.

Witnessed & Understood by me, Date

Invented by Date

Recorded by

Project No._____
Book No._____ TITLE _____

Page No.___

DTL TRIPLETT #4

- used BELL BHT-910 probe #4436 on very thin wooden probe arm.

I) B-I Curves: at ½ bore (.944" ÷ 2 = .472" dia. or X = ± .236") Y = 0.0"

a) Q1 B-I Z = -5.125"

I (amps)	V (volts)	B (KG) Q1 ONLY X = -.236"	.236"	AV.	B(KG.) Q2 at 200A. -.236"	.236"	AV.
25A.	.72V.	-.505	.491	.498	-.513	.497	.505
50	1.63	-1.136	1.109	1.123	-1.143	1.115	1.129
75	2.52	-1.760	1.719	1.740	-1.761	1.724	1.743
100	3.40	-2.350	2.295	2.322	-2.350	2.294	2.322
125	4.29	-2.938	2.865	2.902	-2.938	2.867	2.903
150	5.17	-3.488	3.412	3.450	-3.483	3.395	3.439
175	6.07	-3.977	3.893	3.935	-3.981	3.876	3.929
200	6.98	-4.314	4.212	4.263	-4.306	4.202	4.252
225	7.90	-4.571	4.465	4.518	-4.554	4.446	4.500
200		-4.350	4.235	4.293			91.6%
150		-3.519	3.440	3.480			
100		-2.363	2.314	2.339			
50		-1.151	1.125	1.138			

To Page No.____

Project No._____

TITLE_____ Book No._____

From Page No.___

b) Q3 B-I (Z = 5.125", Y = 0.0")

I (amps)	V (volts)	B (KG.) Q3 ONLY X = +.236"	-.236"	AV.	B (KG.) Q2 at 200A. +.236"	-.236"	AV.
25A	.72 V.	.516	-.493	.505	.523	-.500	.512
50	1.63	1.161	-1.106	1.134	1.172	-1.111	1.142
75	2.52	1.804	-1.717	1.761	1.808	-1.714	1.761
100	3.40	2.409	-2.290	2.350	2.409	-2.288	2.349
125	4.28	3.006	-2.860	2.933	3.004	-2.858	2.931
150	5.16	3.575	-3.397	3.486	3.575	-3.397	3.486
175	6.05	4.079	-3.870	3.975	4.075	-3.857	3.966
200	6.96	4.410	-4.189	4.299	4.415	-4.182	4.299
225	7.87	4.670	-4.448	4.559	4.666	-4.425	4.546
200		4.442	-4.212	4.327			
150		3.614	-3.420	3.517			
100		2.428	-2.302	2.365			
50		1.179	-1.120	1.150			

c) Q2 B-I (Z = 0.0", Y = 0.0")

I (amps)	V (volts)	B (KG.) Q2 ONLY X = -.236"	.236"	AV.	B (KG.) Q1/Q3 at 178A -.236"	.236"	AV.
25A	1.11 V.	.616	-.625	.621	.610	-.628	.619
50	2.22	1.228	-1.245	1.237	1.220	-1.253	1.237
75	3.34	1.841	-1.866	1.854	1.829	-1.876	1.853
100	4.47	2.444	-2.478	2.461	2.427	-2.490	2.459
125	5.62	3.039	-3.090	3.065	3.019	-3.099	3.059
150	6.77	3.610	-3.666	3.638	3.582	-3.689	3.635
175	7.95	4.108	-4.181	4.145	4.082	-4.192	4.137
200	9.15	4.474	-4.553	4.514	4.436	-4.553	4.495
225	10.38	4.737	-4.809	4.773	4.689	-4.822	4.756
250	11.63	4.937	-5.033	4.985	4.897	-5.036	4.967
200		4.488	-4.577	4.533			
150		3.644	-3.734	3.689			
100		2.467	-2.526	2.497			
50		1.252	-1.282	1.267			

To Page No.___

Witnessed & Understood by me,	Date	Invented by	Date
		Recorded by	

B pseudoLangevin fit to Q1-like Quadrupoles

```
iter chisq delta/lim lambda a1 a3
0 9.0872967770e+00 0.00e+00 8.01e-01 1.000000e-02 1.000000e-02
1 1.6023976412e+00 -4.67e+10 8.01e-02 4.340328e-03 6.589126e-03
2 1.3886807750e-02 -1.14e+12 8.01e-03 4.597991e-03 4.671716e-03
3 4.5018042513e-03 -2.08e+10 8.01e-04 4.716700e-03 5.001648e-03
4 4.2847009626e-03 -5.07e+08 8.01e-05 4.717930e-03 4.973124e-03
5 4.2846913243e-03 -2.25e+04 8.01e-06 4.718041e-03 4.973316e-03
* 4.2846913319e-03 1.78e+01 8.01e-05 4.718041e-03 4.973314e-03
* 4.2846913319e-03 1.78e+01 8.01e-04 4.718041e-03 4.973314e-03
* 4.2846913319e-03 1.78e+01 8.01e-03 4.718041e-03 4.973314e-03
* 4.2846913319e-03 1.78e+01 8.01e-02 4.718041e-03 4.973314e-03
* 4.2846913319e-03 1.77e+01 8.01e-01 4.718041e-03 4.973314e-03
* 4.2846913312e-03 1.63e+01 8.01e+00 4.718041e-03 4.973314e-03
* 4.2846913250e-03 1.67e+00 8.01e+01 4.718041e-03 4.973316e-03
* 4.2846913243e-03 1.65e-02 8.01e+02 4.718041e-03 4.973316e-03
* 4.2846913243e-03 1.88e-04 8.01e+03 4.718041e-03 4.973316e-03
6 4.2846913243e-03 -1.42e-05 8.01e+02 4.718041e-03 4.973316e-03
iter chisq delta/lim lambda a1 a3

After 6 iterations the fit converged.
final sum of squares of residuals :  0.00428469
rel.  change during last iteration :  -1.41703e-15

degrees of freedom (FIT_NDF) : 102
rms of residuals (FIT_STDFIT) = sqrt(WSSR/ndf) :  0.00648126
variance of residuals (reduced chisquare) = WSSR/ndf :  4.20068e-05

Final set of parameters Asymptotic Standard Error
======================= ==========================
a1 = 0.00471804 +/- 8.107e-06 (0.1718%)
a3 = 0.00497332 +/- 2.318e-05 (0.4661%)

correlation matrix of the fit parameters:
a1 a3
a1 1.000
a3 0.800 1.000
```

C pseudoLangevin fit to Q2-like Quadrupoles

```
iter chisq delta/lim lambda a1 a3
0 3.7836705967e+00 0.00e+00 8.17e-01 1.000000e-02 1.000000e-02
1 6.9783252667e-01 -4.42e+10 8.17e-02 5.003653e-03 6.693559e-03
2 1.0942852484e-02 -6.28e+11 8.17e-03 4.803584e-03 4.649521e-03
3 1.2903152457e-03 -7.48e+10 8.17e-04 4.955713e-03 4.941091e-03
4 1.2047676108e-03 -7.10e+08 8.17e-05 4.961283e-03 4.932590e-03
5 1.2047644017e-03 -2.66e+04 8.17e-06 4.961228e-03 4.932434e-03
6 1.2047643778e-03 -1.98e+02 8.17e-07 4.961227e-03 4.932431e-03
7 1.2047643774e-03 -3.73e+00 8.17e-08 4.961227e-03 4.932431e-03
8 1.2047643774e-03 -7.21e-02 8.17e-09 4.961227e-03 4.932431e-03
iter chisq delta/lim lambda a1 a3

After 8 iterations the fit converged.
final sum of squares of residuals :  0.00120476
rel.  change during last iteration :  -7.21437e-12

degrees of freedom (FIT_NDF) : 54
rms of residuals (FIT_STDFIT) = sqrt(WSSR/ndf) :  0.00472339
variance of residuals (reduced chisquare) = WSSR/ndf :  2.23105e-05

Final set of parameters Asymptotic Standard Error
======================= ==========================
a1 = 0.00496123 +/- 7.688e-06 (0.155%)
a3 = 0.00493243 +/- 1.668e-05 (0.3381%)


correlation matrix of the fit parameters:
a1 a3
a1 1.000
a3 0.800 1.000
```

D DTL Triplet Quadrupole Wollnik Integrals

Each DTL triplet had its magnetic fields measured by Doug Evans, circa 2000, with the first triplet measured during March 2000, up to the final triplet in September of the same year. The original measurement files, backed up on `lin12.triumf.ca` have been recovered and analyzed, allowing for both the B-I parametrization, in addition to Enge function fits, producing magnet effective lengths, to be performed.

The source files consituting the raw data are listed in Table 5. Measurements used for this work came in two typical set formats: (1) both outer quadrupoles powered, with the central quad off, and (2) both outer quadrupoles off, central quadrupole powered. This is signitifant, as the DTL triplet quadrupoles are sufficiently proximate to each other to render fitting their magnetic field profiles challenging. An example measurement, not used for fringe field parameter extraction, in which

each quadrupole is powered, is shown in Figure 18.

File	Triplet	Outer Q. Cur. [A]	Inner Q. Cur. [A]
030700.3	Q1,Q2,Q3	178	0
031400.3	Q1,Q2,Q3	0	200
20000706.3	Q4,Q5,Q6	178	0
20000706.4	Q4,Q5,Q6	0	200
20000908.4	Q7,Q8,Q9	178	0
20000908.5	Q7,Q8,Q9	0	200
20000929.3	Q10,Q11,Q12	178	0
20000929.4	Q10,Q11,Q12	0	200

Table 5: Summary of DTL quadrupole triplet magnetic field surveys, including source datafile and quadrupole setpoints for each. All surveys listed above are taken with the steering coils powered off. All data obtained from Rick Baartman.

By selecting datafiles shown in Table 5, it is possible to isolate individual quadrupoles from the triplet, thereby obtaining magnetic field fall-off profiles which are unperturbed by the unpowered neighbouring quadrupole. In cases where the central quad is unpowered, the separation between outer triplet quadrupoles is sufficient to allow the magnetic fields to return to measurement noise levels well before the effect of the opposite element is seen. An example of this, for the first DTL triplet, is shown in Figure 19.

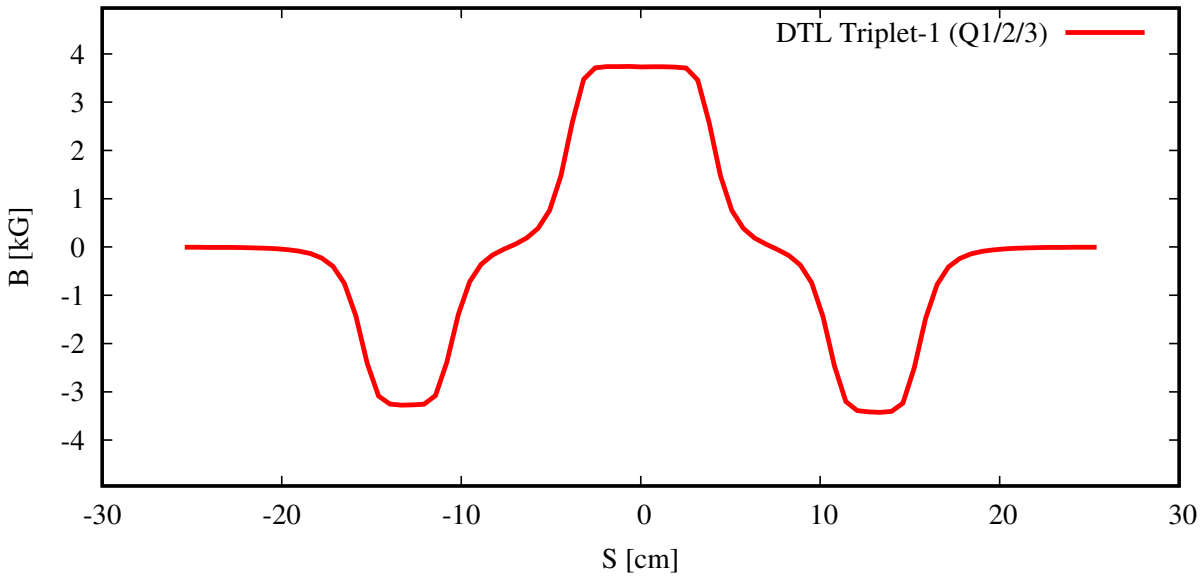

Figure 18: Quadrupole triplet magnetic field measurement, for x = 0.0”, y = -0.200” (both held fixed) versus s, the optical axis through the triplet. Performed by Doug Evans, 2000, datafile 031500.1, March 15, 2000.

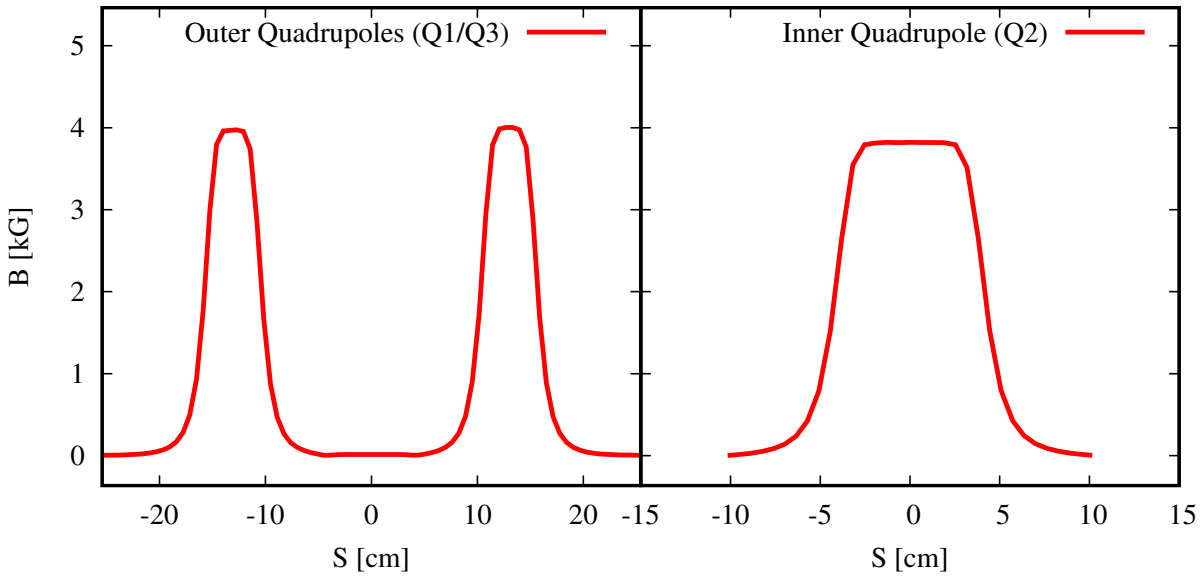

Figure 19: Sample slices taken from (L) `030700.3` for Q1/Q3 and (R) `031400.3` for Q2, showing the magnetic field strength vs. position along the optical axis through the triplet. Observe how the Q1,Q2 and Q3 fields overlap in the regions bounded by (-10cm;-5cm) and (5cm;10cm) in Figure 18 noticably overlap, while in the present figure each quad may be treated separately.

Quadrupole Fringe Field Integrals

A symmetric quadrupole field can be fit to:

$$E(s) = k_0\Big[E\big(L/2+s\big) + E\big(L/2-s\big) - 1\Big] \tag{2}$$

Where $E(s)$ is an edge function, fit to the (symmetric) quadrupole fringe fields along the optical axis. Typically, fringe fields for long magnetic quadrupoles, with a diameter D smaller than the length L, are represented with an Enge function, of the form:

$$E(s) = \frac{1}{1+e^{P(s)}} P(s) = \sum_{i=0}^{5} a_k \big(\frac{-s}{D}\big)^k$$

Statistically, fitting fringe fields to the above, which features 6 fit parameters, is a tricky exercise, due in no small part to the high sensitivity of the fit parameters to noise. Baartman and Kaltchev have parametrized short quadrupoles using a one-parameter fit tan-hyperbolic definition to the Enge

fringe field edge function [2] for a quadrupole diameter D:

$$E(s) = \frac{1 + \tanh\left(\frac{a_1 s}{2D}\right)}{2} \tag{3}$$

Matsuda and Wollnik have introduced a set of four fringe field integrals [2, 3]:

$$I_1 \equiv \int_0^s \int E(s)dsds - s^2/2 = \frac{4\zeta(2)}{a_1^3} \tag{4}$$

$$I_2 \equiv \int_0^s s \int E(s)dsds - s^3/3 = 0 \tag{5}$$

$$I_3 \equiv \int_0^s \left(\int E(s)ds\right)^2 ds - sb^3/3 = \frac{16\zeta(3)}{a_1^3} \tag{6}$$

$$I_4 \equiv \int_0^s E(s)^2 ds - s = -\frac{2}{a_1} \tag{7}$$

where ζ is the Riemann Zeta function. In the words of Matsuda and Wollnik:

> *These I_1,...,I_4 are defined so that the values are independent of z_b[2] for any real fringing field if z_b is some point in the main field region because in this region we have the relationship*

$$\int_{z_a}^{z} k(z)dz = k_0 z, \quad \text{for} \quad z \gtrsim z_b \tag{8}$$

The integrals I_1 to I_4 present the advantage of being independent of the integration bounds [3]. Conversely, the Enge polynomial (3), with up to fifth order of s, is potentially extremely sensitive to noise in the field profile data. In the Baartman/Kaltchev definition of Eq. (3), which supposes symmetric fringe fields, only the Enge coefficient a_1 is kept nonzero for the fit. This simultaneously allows for the evaluation of the fringe field integrals, but for short quadrupoles it also produces a simple strength function:

$$k(s) = \frac{k_0}{2}\left[\tanh\left(a_1(L/2 + s)\right) + \tanh\left(L/2 - 2\right)\right] \tag{9}$$

finally, it is noted that the effective length L is related to k_0 via:

$$\int k(s)ds = k_0 L \tag{10}$$

[2] in the present note, the variable z_b is written as s, the distance along the optical axis.

The magnetic field survey files in Table 5 were used to evaluate the integrals $I_1, ..., I_4$ for the each DTL quadrupole triplet, with the results listed in Table 6. Averaged values for each quadrupole type are shown in Table 7.

Quadrupole	I_1	I_2	I_3	I_4	L [inch]
DTL:Q1	0.5037	−0.2417	0.2208	−0.5259	2.307
DTL:Q2	0.4410	−0.2305	0.1617	−0.4828	3.485
DTL:Q3	0.4947	−0.2421	0.2119	−0.5195	2.299
DTL:Q4	0.5030	−0.2512	0.2161	−0.5233	2.294
DTL:Q5	0.4517	−0.2304	−0.1719	−0.491	3.486
DTL:Q6	0.4862	−0.2182	0.2131	−0.5195	2.288
DTL:Q7	0.4916	−0.2391	0.2092	−0.5180	2.312
DTL:Q8	0.4552	−0.2323	0.1748	−0.4932	3.485
DTL:Q9	0.4938	−0.2498	0.2078	−0.5171	2.337
DTL:Q10	0.4908	−0.2501	0.2046	−0.5149	2.294
DTL:Q11	0.4538	−0.2331	0.1730	−0.4919	3.490
DTL:Q12	0.5025	−0.2308	0.2240	−0.5276	2.334

Table 6: Fringe field integrals for the DTL triplet quadrupoles, evaluated on magnetic field survey data listed in Table 5.

Quadrupole	I_1	I_2	I_3	I_4	L [inch]
Outer	0.4958	−0.2404	0.2134	−0.5207	2.231
Inner	0.4504	−0.2316	0.1698	−0.4897	3.487

Table 7: Averaged fringe field integrals for the DTL triplet quadrupoles, evaluated on magnetic field survey data listed in Table 5. Quadrupoles were grouped as outer quadrupoles (Q1/Q3, Q4/5, Q6/7, Q9/10, Q12) and Inner quadrupoles (Q2, Q5, Q8, Q11).

References

[1] R.E. Laxdal. *Concept Design for Quadrupole Triplets for the ISAC Separated Function Drift Tube Linac*. Technical Report TRI-DN-99-05, TRIUMF, 1999.

[2] R Baartman and D Kaltchev. *Short quadrupole parametrization*. In *2007 IEEE Particle Accelerator Conference (PAC)*, pages 3229–3231. IEEE, 2007.

[3] H Matsuda and H Wollnik. Third order transfer matrices for the fringing field of magnetic and electrostatic quadrupole lenses. *Nuclear Instruments and Methods*, 103(1):117–124, 1972.